# ELASTIC BUCKLING OF A SIMPLY SUPPORTED RECTANGULAR SANDWICH PANEL SUBJECTED TO COMBINED EDGEWISE BENDING, COMPRESSION, AND SHEAR

No. 1859

November 1956



**This Report is One of a Series Issued in Cooperation with the ANC-23 PANEL ON SANDWICH CONSTRUCTION of the Departments of the AIR FORCE, NAVY, AND COMMERCE**

FOREST PRODUCTS LABORATORY
MADISON 5, WISCONSIN

UNITED STATES DEPARTMENT OF AGRICULTURE
FOREST SERVICE
In Cooperation with the University of Wisconsin

# ELASTIC BUCKLING OF A SIMPLY SUPPORTED RECTANGULAR SANDWICH PANEL SUBJECTED TO COMBINED EDGEWISE BENDING, COMPRESSION, AND SHEAR[1]

By

W. R. KIMEL, Engineer

Forest Products Laboratory,[2] Forest Service
U. S. Department of Agriculture

---

## Summary

This paper presents a theoretical analysis of the problem of the elastic buckling of simply supported rectangular sandwich panels acted upon by combinations of edgewise bending, compression, and shear. The mathematical solution of the problem is based upon the Rayleigh-Ritz energy method. Design curves are presented for determining the buckling criteria for panels loaded in combined edgewise bending and shear.

## Introduction

The problem of the elastic buckling of simply supported rectangular sandwich panels subjected to combined edgewise bending and compression was solved in Forest Products Laboratory Reports Nos. 1857 and 1857-A.

---

[1] This report is one of a series (ANC-23, Item 56-5) prepared and distributed by the Forest Products Laboratory under U. S. Navy, Bureau of Aeronautics Nos. NAer 01684 and NAer 01593 and U. S. Air Force No. DO 33(616)-56-9. Results here reported are preliminary and may be revised as additional data become available.

[2] Maintained at Madison, Wis., in cooperation with the University of Wisconsin.

It is the purpose of this paper to present an analysis for the problem of the elastic buckling of simply supported rectangular sandwich panels subjected to combined edgewise bending, compression, and shear.

Many aircraft structural components that are constructed of sandwich are required to carry combinations of edgewise bending, compression, and shear loading. Examples of such components are the division bulkheads in cellular-type wing structures, and trailing edge wing panels. Data useful for the design of such components are presented in this paper by curves. These data are for use in calculating buckling loads on panels subjected to combinations of edgewise bending and shear. Formulas are developed from which buckling criteria for any combination of edgewise bending, compression, and shear may be calculated.

The solution utilizes the same assumptions used in Forest Products Laboratory Reports Nos. 1857 and 1857-A. The sandwich panel is assumed to be composed of isotropic thin plate facings of either equal or unequal thickness and of either an isotropic or an orthotropic core. The core is assumed to be in a state of antiplane stress. The mathematical analysis employed here is also identical in principle with that used in Forest Products Laboratory Reports Nos. 1857 and 1857-A. More specifically, the mathematical solution is based on a Rayleigh-Ritz energy method using double Fourier series with configuration parameters obtained from solutions of the core equilibrium equations. The configuration parameters are constants of integration obtained from solution of the core equilibrium equations. The general literal solution to this problem is in the form of a characteristic determinant of order infinity, except in the special case of pure edgewise compression, in which case the determinant is of order six.[3]

Evaluation of an order 48 minor from the determinant of order infinity is made to obtain data for design curves. These design curves, based on the additional assumption of an infinite transverse modulus of elasticity of the core, $E_c$, and on a modified flexural rigidity of the spaced facings,[4] are compiled for the case of combined edgewise bending and shear. The transverse modulus of elasticity of the core refers to the modulus of

---

[3] This determinant is given in equation (179) of reference (2). Underlined numbers in parentheses refer to Literature Cited at the end of this report.

[4] These assumptions, $E_c = \infty$ and $D_T = D$, were used to obtain the literal solutions from which the data for the design curves in references (2) and (3) were computed.

elasticity of the core in a direction perpendicular to the facings. The design curves are believed sufficiently accurate for use in the design of many sandwich panels. The design curves are limited to panel ratios $0.4 \leq \frac{a}{b} \leq 2.0$ and to values of the parameter $W$ depending on values of both the ratios $\frac{a}{b}$ and $\frac{G_{xz}}{G_{yz}}$. Accurate design curves for additional ranges of parameters, $\frac{a}{b}$ and $W$, can be obtained from consideration of a larger set of equations[5] from the infinite set[6] presented in this paper.

## Notation

| | |
|---|---|
| x, y, z | rectangular coordinates (fig. 1) |
| a | length of panel in direction of loading (figs. 1, 3) |
| b | width of panel in direction perpendicular to loading (figs. 1, 3) |
| $\beta$ | $\frac{a}{b}$ |
| c | thickness of core (fig. 1) |
| t | thickness of upper facing (fig. 1) |
| t' | thickness of lower facing (fig. 1) |
| $\mu$ | Poisson's ratio of facings |
| E | modulus of elasticity of facings |
| $E_c$ | modulus of elasticity of core in z direction -- transverse modulus of elasticity of core |
| $G_{xz}$ | modulus of rigidity of core in xz plane |

[5] In this paper 48 linear, homogeneous equations in 48 unknowns were solved.

[6] Equations 20, 21, 22, 23, 24, and 25 constitute this set.

$G_{yz}$ modulus of rigidity of core in yz plane

$r$ $\frac{G_{xz}}{G_{yz}}$

$N_b$ maximum value of normal edgewise loading (load per unit width, b, of panel) due to pure edgewise bending (fig. 4)

$N_c$ value of normal edgewise loading (load per unit width, b, of panel) due to pure edgewise compression (fig. 4)

$N_o$ $N_b + N_c$ (fig. 4)

$N_s$ value of edgewise shear load (load per unit length of edges, a and b, of panel)(fig. 3)

$N_{ocr}$ value of $N_o$ at buckling

$M_{ocr}$ critical value of edgewise bending moment, $\frac{N_o b^2}{6}$

$N_{scr}$ value of $N_s$ at buckling

$\alpha$ $\frac{2N_b}{N_o}$ (figs. 3, 4)

u, v, w displacements of upper facing in x, y, and z directions, respectively

u', v', w' displacements of lower facing in x, y, and z directions, respectively

$u_c$, $v_c$, $w_c$ displacements of core in x, y, and z directions, respectively

m, n, p, q, i integers

$A_{mn}$, $B_{mn}$, $C_{mn}$, $D_{mn}$, $E_{mn}$, $G_{mn}$ configuration parameters -- also constants of integration from core equations

V elastic potential energy of panel with respect to undeflected configuration of panel

$T$ potential energy of system of edgewise loads with respect to undeflected configuration of panel

$\delta$ $\dfrac{E\pi^2}{c\,(1-\mu^2)}$

$\theta_{mn}$ $\dfrac{m^2}{a^2} + \dfrac{n^2}{b^2}$

$\Phi_{mn}$ $m^2 + n^2\beta^2$

$\Lambda_{mn}$ $m^2 + \dfrac{n^2\beta^2}{r}$

$\Omega_{mn}$ $\dfrac{\pi^2}{32\beta}\left[\dfrac{\Phi_{mn}^2}{\beta^2} D'_{mn} - \dfrac{m^2}{\pi^2} N_{ocr}\, b^2 \left(1 - \dfrac{\alpha}{2}\right)\right]$

$\Psi_{mn}$ $\dfrac{\pi^2}{32\beta}\left[\dfrac{\Phi_{mn}^2 J_{mn}}{\beta^2} - m^2 k_\alpha \left(1 - \dfrac{\alpha}{2}\right)\right]$

$J_{mn}$ $$\frac{1}{1 + \dfrac{W}{\beta^2}\dfrac{\Phi_{mn}^2}{\Lambda_{mn}} + \dfrac{n^2 m^2 r W \left(1 - \frac{1}{r}\right)^2}{\Lambda_{mn}\left(1 + \Lambda_{mn}\dfrac{W}{\beta^2}\dfrac{1-\mu}{2} r\right)}}$$

$D'_{mn}$ $$\frac{E}{1-\mu^2}\left[I_F + \frac{I_T}{1 + \dfrac{W}{\beta^2}\dfrac{\Phi_{mn}^2}{\Lambda_{mn}} + \dfrac{n^2 m^2 r W \left(1 - \frac{1}{r}\right)^2}{\Lambda_{mn}\left(1 + \Lambda_{mn}\dfrac{W}{\beta^2}\dfrac{1-\mu}{2} r\right)}}\right]$$

$k_\alpha$ critical load factor corresponding to loading defined by $\underline{\alpha}$, $\frac{N_{ocr}\, b^2}{D_T\, \pi^2}$

$k_2$ critical load factor corresponding to pure edgewise bending, $\frac{N_{ocr}\, b^2}{D_T\, \pi^2}$

$k_s$ critical load factor corresponding to pure edgewise shear, $\frac{N_{scr}\, b^2}{D_T\, \pi^2}$

$P_{p,q}$ elements of determinant

$I_F$ $\frac{t^3 + (t')^3}{12}$

$I_T$ $\frac{tt'}{t + t'} \left(c + \frac{t + t'}{2}\right)^2$

$I$ $I_F + I_T$

$D$ $\frac{EI}{1-\mu^2}$

$D_T$ $\frac{EI_T}{1-\mu^2}$

$W$ $\frac{ctt'}{t + t'} \frac{\pi^2}{b^2} \frac{E}{1-\mu^2} \frac{1}{G_{xz}}$

## Mathematical Analysis

The sandwich panel with its relation to the coordinate axes $x$, $y$, and $z$ is shown in figure 1. The sandwich core is assumed to be in a state of stress distribution that has been defined as antiplane stress.[7] A free body diagram of an element of the core is shown in figure 2. The facings are treated in accordance with isotropic thin plate theory.

Displacement functions which satisfy equilibrium of the core were derived in detail in reference (2) and are as follows:

$$u_c = -\sum_{m=1}^{\infty}\sum_{n=1}^{\infty} \frac{m\pi}{a}\left[A_{mn}\frac{z^3}{6} + B_{mn}\frac{z^2}{2} + F_{mn}\,z + G_{mn}\right] \times \cos\frac{m\pi x}{a}\,\sin\frac{n\pi y}{b} \tag{1}$$

$$v_c = -\sum_{m=1}^{\infty}\sum_{n=1}^{\infty} \frac{n\pi}{b}\left[A_{mn}\frac{z^3}{6} + B_{mn}\frac{z^2}{2} + D_{mn}\,z + E_{mn}\right] \times \sin\frac{m\pi x}{a}\,\cos\frac{n\pi y}{b} \tag{2}$$

and

$$w_c = \sum_{m=1}^{\infty}\sum_{n=1}^{\infty}\left[A_{mn}\frac{z^2}{2} + B_{mn}\,z + C_{mn}\right]\sin\frac{m\pi x}{a}\,\sin\frac{n\pi y}{b} \tag{3}$$

where the constants $A_{mn}$, $C_{mn}$, $D_{mn}$, and $F_{mn}$ are related by equation (26) of reference (2).

These displacement functions permit a derivation of the elastic energy, $V$, of the simply supported sandwich panel associated with a small

[7] Antiplane stress is defined in reference (2).

deflected configuration of the panel. This elastic (potential) energy, V, of the simply supported panel is given by equation (154) of reference (2).

The potential energy, T, of the edge loads with respect to the undeflected configuration of the panel is derived in the same manner as in reference (2). The expression for normal edge load, $N_o\left(1 - \frac{\alpha y}{b}\right)$ (load per unit width, b, of panel), makes possible a general solution for critical load of a panel subjected to any combination of edgewise bending and compression. The numerical value of $\alpha$ defines the nature of the normal edgewise loading. The shear edge load is denoted by $N_s$ (load per unit length of edges a and b of the panel). $\alpha$, $N_o$, and $N_s$ are further defined in figures 3 and 4. The core has been assumed to be incapable of carrying loads in directions parallel to the facings,[8] therefore the edge loads must be mathematically applied to the facings. The stresses in both facings will be the same for facings of like materials. Thus the potential energy, T, is given by the equation

$$T = \frac{1}{2}\int_0^a\int_0^b \frac{N_o}{t + t'}\left(1 - \frac{\alpha y}{b}\right)\left[t\left(\frac{\partial w}{\partial x}\right)^2 + t'\left(\frac{\partial w'}{\partial x}\right)^2\right] dx\, dy$$

$$- \frac{1}{2}\int_0^a\int_0^b \frac{2N_s}{t + t'}\left[t\,\frac{\partial w}{\partial x}\,\frac{\partial w}{\partial y} + t'\,\frac{\partial w'}{\partial x}\,\frac{\partial w'}{\partial y}\right] dx\, dy \qquad (4)$$

where $\frac{\partial w}{\partial x}$ and $\frac{\partial w}{\partial y}$ refer to the slopes of the upper facing in the xz and yz planes, respectively, and $\frac{\partial w'}{\partial x}$ and $\frac{\partial w'}{\partial y}$ refer to the slopes of the lower facing in the xz and yz planes, respectively.

Equation (4) is now written as

$$T = T_1 + T_2 \qquad (5)$$

---

[8] This follows directly from the assumption that the stress distribution in the core is antiplane.

where

$$T_1 = \frac{1}{2} \int_0^a \int_0^b \frac{N_o}{t + t'} \left(1 - \frac{\alpha y}{b}\right) \left[ t \left(\frac{\partial w}{\partial x}\right)^2 + t' \left(\frac{\partial w'}{\partial x}\right)^2 \right] dx\, dy$$

and

$$T_2 = -\frac{1}{2} \int_0^a \int_0^b \frac{2N_s}{t + t'} \left[ t \frac{\partial w}{\partial x} \frac{\partial w}{\partial y} + t' \frac{\partial w'}{\partial x} \frac{\partial w'}{\partial y} \right] dx\, dy$$

The integrated form of $T_1$ is given in equation (166) of reference (2). The integrated form of $T_2$ can be written by noting that

$$\int_0^a \sin \frac{m\pi x}{a} \cos \frac{p\pi x}{a}\, dx = 0, \tag{6}$$

when $m \pm p$ is even, that

$$\int_0^a \sin \frac{m\pi x}{a} \cos \frac{p\pi x}{a}\, dx = \frac{2a}{\pi} \frac{m}{m^2 - p^2} \tag{7}$$

when $m \pm p$ is odd, and from equations (1), (2), and (3) that

$$\frac{\partial w}{\partial x} = \left.\frac{\partial w_c}{\partial x}\right|_{z=0} = \sum_{m=1}^{\infty} \sum_{n=1}^{\infty} C_{mn} \frac{m\pi}{a} \cos \frac{m\pi x}{a} \sin \frac{n\pi y}{b} \tag{8}$$

$$\frac{\partial w}{\partial y} = \left.\frac{\partial w_c}{\partial y}\right|_{z=0} = \sum_{m=1}^{\infty} \sum_{n=1}^{\infty} C_{mn} \frac{n\pi}{b} \sin \frac{m\pi x}{a} \cos \frac{n\pi y}{b} \tag{9}$$

$$\frac{\partial w'}{\partial x} = \frac{\partial w_c}{\partial x}\bigg|_{z=c} = \sum_{m=1}^{\infty} \sum_{n=1}^{\infty} \left(A_{mn} \frac{c^2}{2} + B_{mn}\, c + C_{mn}\right) \frac{m\pi}{a}$$

$$\times \cos \frac{m\pi x}{a} \sin \frac{n\pi y}{b} \tag{10}$$

and

$$\frac{\partial w'}{\partial y} = \frac{\partial w_c}{\partial y}\bigg|_{z=c} = \sum_{m=1}^{\infty} \sum_{n=1}^{\infty} \left(A_{mn} \frac{c^2}{2} + B_{mn}\, c + C_{mn}\right) \frac{n\pi}{b}$$

$$\times \sin \frac{m\pi x}{a} \cos \frac{n\pi y}{b} \tag{11}$$

Therefore,

$$T_2 = -\frac{4N_s}{t + t'} \sum_{m}^{\infty} \sum_{n}^{\infty} \sum_{p}^{\infty} \sum_{q}^{\infty} \frac{mnpq}{(m^2 - p^2)(q^2 - n^2)} \left[ C_{mn}\, C_{pq}\, t \right.$$

$$\left. + \left(A_{mn} \frac{c^2}{2} + B_{mn}\, c + C_{mn}\right)\left(A_{pq} \frac{c^2}{2} + B_{pq}\, c + C_{pq}\right) t' \right] \tag{12}$$

where $\underline{m} \pm \underline{p}$ and $\underline{n} \pm \underline{q}$ are odd.

The complete expression for $\underline{T}$ can now be written as follows:

$$T = \frac{N_o ab}{8(t + t')} \sum_{m=1}^{\infty} \sum_{n=1}^{\infty} \frac{m^2 \pi^2}{a^2} \left\{ \left[ t\, C_{mn}^2 + t' \left( A_{mn} \frac{c^2}{2} + B_{mn}\, c + C_{mn} \right)^2 \right] \left[ 1 - \frac{\alpha}{2} \right] \right.$$

$$+ \frac{8\alpha}{\pi^2} \sum_{i}^{\infty} \left[ t\, C_{mn}\, C_{mi} + t' \left( A_{mn} \frac{c^2}{2} + B_{mn}\, c + C_{mn} \right) \left( A_{mi} \frac{c^2}{2} + B_{mi}\, c + C_{mi} \right) \right]$$

$$\left. \times \frac{ni}{(n^2 - i^2)^2} \right\} - \frac{4N_s}{t + t'} \sum_{m}^{\infty} \sum_{n}^{\infty} \sum_{p}^{\infty} \sum_{q}^{\infty} \frac{mnpq}{(m^2 - p^2)(q^2 - n^2)} \left[ C_{mn}\, C_{pq}\, t \right.$$

$$\left. + \left( A_{mn} \frac{c^2}{2} + B_{mn}\, c + C_{mn} \right) \left( A_{pq} \frac{c^2}{2} + B_{pq}\, c + C_{pq} \right) t' \right] \qquad (13)$$

where $\underline{m} \pm \underline{p}$, $\underline{n} \pm \underline{q}$, and $\underline{i} \pm \underline{n}$ are odd.

For a condition of instability, the total energy of the system, $\underline{V} - \underline{T}$, must have a stationary value with respect to any arbitrary change in configuration of the system. The configuration of this system is defined by the parameters $\underline{A_{mn}}$, $\underline{B_{mn}}$, ... , $\underline{G_{mn}}$. These parameters also serve as constants of integration and were obtained from solutions of the core equilibrium equations.[9] Thus, at the incipience of buckling, it is necessary that

$$\frac{\partial V}{\partial A_{mn}} - \frac{\partial T}{\partial A_{mn}} = 0 \tag{14}$$

$$\frac{\partial V}{\partial B_{mn}} - \frac{\partial T}{\partial B_{mn}} = 0 \tag{15}$$

$$\frac{\partial V}{\partial C_{mn}} - \frac{\partial T}{\partial C_{mn}} = 0 \tag{16}$$

$$\frac{\partial V}{\partial D_{mn}} - \frac{\partial T}{\partial D_{mn}} = 0 \tag{17}$$

$$\frac{\partial V}{\partial E_{mn}} - \frac{\partial T}{\partial E_{mn}} = 0 \tag{18}$$

and

$$\frac{\partial V}{\partial G_{mn}} - \frac{\partial T}{\partial G_{mn}} = 0 \tag{19}$$

---

[9] The constants $\underline{A_{mn}}$, $\underline{B_{mn}}$, ... , $\underline{G_{mn}}$ are all identically zero, for the loadings considered in this paper, prior to the incipience of buckling.

Substitutions of V from equation (154) of reference (2) and of T from equation (13) into each of equations (14), (15), (16), (17), (18), and (19) yield, respectively,

$$E_c\left(\frac{A_{mn}c^2}{3}+\frac{B_{mn}c}{2}\right)+\frac{E_c}{G_{xz}}\frac{a^2}{m^2\pi^2}\left[G_{yz}\frac{n^2\pi^2}{b^2}(D_{mn}-C_{mn})+E_c A_{mn}\right]+\frac{c^2\delta\pi^2}{24}\theta_{mn}^2(t')^3\left(A_{mn}\frac{c^2}{2}\right.$$

$$\left.+B_{mn}c+C_{mn}\right)+t'\delta\pi^2\left\{\left[\theta_{mn}\left(\frac{c^3}{6}+\frac{c^2t'}{4}\right)A_{mn}+\theta_{mn}\left(\frac{c^2+ct'}{2}\right)B_{mn}+\frac{\theta_{mn}t'}{2}C_{mn}+\frac{m^2}{a^2}\rho_{mn}c\,C_{mn}\right.\right.$$

$$\left.-\frac{E_c}{G_{xz}}\frac{c}{\pi^2}A_{mn}+\frac{n^2}{b^2}c\left(1-\frac{1}{r}\right)D_{mn}+\frac{m^2}{a^2}G_{mn}+\frac{n^2}{b^2}E_{mn}\right]\left[\theta_{mn}\left(\frac{c^3}{6}+\frac{c^2t'}{4}\right)-\frac{E_c c}{G_{xz}\pi^2}\right]-\frac{n^2}{b^2\pi^2}\frac{E_c}{G_{xz}}\frac{1-\mu}{2}$$

$$\left.\times\left[c^2\rho_{mn}(C_{mn}-D_{mn})-\frac{E_c}{G_{xz}}\frac{a^2}{m^2\pi^2}c^2A_{mn}+c(G_{mn}-E_{mn})\right]\right\}-\frac{N_o t'}{2(t+t')}\frac{m^2\pi^2}{a^2}c\left[\left(A_{mn}\frac{c^2}{2}\right.\right.$$

$$\left.\left.+B_{mn}c+C_{mn}\right)\left(1-\frac{\alpha}{2}\right)+\frac{8\alpha}{\pi^2}\sum_i^{\infty}\left(A_{mi}\frac{c^2}{2}+B_{mi}c+C_{mi}\right)\frac{ni}{(n^2-i^2)^2}\right]$$

$$+\frac{16ct'}{ab(t+t')}N_s\,mn\sum_p^{\infty}\sum_q^{\infty}\frac{pq}{(m^2-p^2)(q^2-n^2)}\left(A_{pq}\frac{c^2}{2}+B_{pq}c+C_{pq}\right)=0 \qquad (20)$$

$$E_c \left(A_{mn} \frac{c}{2} + B_{mn}\right) + \frac{\delta \pi^2 \theta_{mn}^2 c (t')^3}{12} \left(A_{mn} \frac{c^2}{2} + B_{mn}\, c + C_{mn}\right) + t' \delta \pi^2 \left\{ \left[ \theta_{mn} \left(\frac{c^3}{6} + \frac{c^2 t'}{4}\right) A_{mn} \right.\right.$$

$$+ \theta_{mn} \left(\frac{c^2 + ct'}{2}\right) B_{mn} + \frac{\theta_{mn} t'}{2} C_{mn} + \frac{m^2}{a^2} \rho_{mn}\, c\, C_{mn} - \frac{E_c}{G_{xz}} \frac{c}{2} \frac{}{\pi} A_{mn} + \frac{n^2}{b^2} c \left(1 - \frac{1}{r}\right) D_{mn}$$

$$\left. \left. + \frac{m^2}{a^2} G_{mn} + \frac{n^2}{b^2} E_{mn} \right] \left[ \theta_{mn} \left(\frac{c^2 + ct'}{2}\right) \right] \right\} - \frac{N_o t'}{t + t'} \frac{m^2 \pi^2}{a^2} \left[ \left(A_{mn} \frac{c^2}{2} + B_{mn}\, c + C_{mn}\right) \right.$$

$$\left. \times \left(1 - \frac{\alpha}{2}\right) + \frac{8\alpha}{\pi^2} \sum_{i}^{\infty} \left(A_{mi} \frac{c^2}{2} + B_{mi}\, c + C_{mi}\right) \frac{ni}{\left(n^2 - i^2\right)^2} \right]$$

$$+ \frac{32}{ab} \frac{t'}{t + t'} N_s\, mn \sum_{p}^{\infty} \sum_{q}^{\infty} \frac{pq}{(m^2 - p^2)(q^2 - n^2)} \left(A_{pq} \frac{c^2}{2} + B_{pq}\, c + C_{pq}\right) = 0 \qquad (21)$$

$$G_{yz}\frac{n^2\pi^2}{b^2}\rho_{mn}(C_{mn}-D_{mn})-\frac{1}{r}\frac{a^2}{m^2}\frac{n^2}{b^2}E_c A_{mn}+\frac{\delta\pi^2\theta_{mn}^2}{12}\left[t^3 C_{mn}+(t')^3\left(A_{mn}\frac{c^2}{2}+B_{mn}c+C_{mn}\right)\right]$$

$$+t\delta\pi^2\left[\frac{m^2}{a^2}G_{mn}+\frac{n^2}{b^2}E_{mn}-\frac{t}{2}\theta_{mn}C_{mn}\right]\left[-\frac{t}{2}\theta_{mn}\right]+t'\delta\pi^2\left\{\left[\theta_{mn}\left(\frac{c^3}{6}+\frac{c^2t'}{4}\right)A_{mn}\right.\right.$$

$$+\theta_{mn}\left(\frac{c^2+ct'}{2}\right)B_{mn}+\frac{\theta_{mn}t'}{2}C_{mn}+\frac{m^2}{a^2}\rho_{mn}c\,C_{mn}-\frac{E_c}{G_{xz}}\frac{c}{\pi^2}A_{mn}+\frac{n^2}{b^2}c\,D_{mn}\left(1-\frac{1}{r}\right)+\frac{m^2}{a^2}G_{mn}$$

$$\left.+\frac{n^2}{b^2}E_{mn}\right]\left[\frac{\theta_{mn}t'}{2}+\frac{m^2}{a^2}\rho_{mn}c\right]+\frac{m^2}{a^2}\frac{n^2}{b^2}\frac{1-\mu}{2}\left[c^2\rho_{mn}^2(C_{mn}-D_{mn})-\frac{E_c}{G_{xz}}\frac{a^2}{m^2\pi^2}c^2\rho_{mn}A_{mn}\right.$$

$$\left.\left.+c\rho_{mn}(G_{mn}-E_{mn})\right]\right\}-\frac{N_o}{c(t+t')}\frac{m^2\pi^2}{a^2}\left\{\left[C_{mn}t+\left(A_{mn}\frac{c^2}{2}+B_{mn}c+C_{mn}\right)t'\right](1-\frac{\alpha}{2})\right.$$

$$\left.+\frac{8\alpha}{\pi^2}\sum_i^{\infty}\left[C_{mi}t+\left(A_{mi}\frac{c^2}{2}+B_{mi}c+C_{mi}\right)t'\right]\frac{ni}{(n^2-i^2)^2}\right\}+\frac{32}{abc(t+t')}N_{s\,mn}\sum_p^{\infty}\sum_q^{\infty}\frac{pq}{(m^2-p^2)(q^2-n^2)}$$

$$\times\left[C_{pq}t+\left(A_{pq}\frac{c^2}{2}+B_{pq}c+C_{pq}\right)t'\right]=0 \qquad (22)$$

$$- G_{yz} \frac{n^2\pi^2}{b^2} \rho_{mn} (C_{mn} - D_{mn}) + E_c A_{mn} \frac{G_{yz}}{G_{xz}} \frac{a^2}{m^2} \frac{n^2}{b^2} + t' \delta \pi^2 \left\{ \left[ \theta_{mn} \left( \frac{c^3}{6} + \frac{c^2 t'}{4} \right) A_{mn} \right. \right.$$

$$+ \theta_{mn} \left( \frac{c^2 + ct'}{2} \right) B_{mn} + \theta_{mn} \frac{t'}{2} C_{mn} + \frac{m^2}{a^2} \rho_{mn} c C_{mn} - \frac{E_c}{G_{xz}} \frac{c}{\pi^2} A_{mn} + \frac{n^2}{b^2} c \left(1 - \frac{1}{r}\right) D_{mn}$$

$$\left. + \frac{m^2}{a^2} G_{mn} + \frac{n^2}{b^2} E_{mn} \right] \left[ \frac{n^2}{b^2} c \left(1 - \frac{1}{r}\right) \right] + \frac{m^2}{a^2} \frac{n^2}{b^2} \frac{1-\mu}{2} \left[ c^2 \rho_{mn}^2 (D_{mn} - C_{mn}) \right.$$

$$\left. \left. + \frac{E_c}{G_{xz}} \frac{a^2}{m^2 \pi^2} c^2 \rho_{mn} A_{mn} + c \rho_{mn} (E_{mn} - G_{mn}) \right] \right\} = 0 \qquad (23)$$

$$t\delta\pi^2 \left[ \left( \frac{m^2}{a^2} G_{mn} + \frac{n^2}{b^2} E_{mn} - \frac{t}{2} \theta_{mn} C_{mn} \right) \frac{n^2}{b^2} + \frac{m^2}{a^2} \frac{n^2}{b^2} \frac{1-\mu}{2} (E_{mn} - G_{mn}) \right] + t'\delta\pi^2$$

$$\times \left\{ \left[ \theta_{mn} \left( \frac{c^3}{6} + \frac{c^2 t'}{4} \right) A_{mn} + \theta_{mn} \left( \frac{c^2 + ct'}{2} \right) B_{mn} + \frac{\theta_{mn} t'}{2} C_{mn} + \frac{m^2}{a^2} \rho_{mn} c C_{mn} \right.\right.$$

$$\left.\left. - \frac{E_c}{G_{xz}} \frac{c}{\pi^2} A_{mn} + \frac{n^2}{b^2} c \left(1 - \frac{1}{r}\right) D_{mn} + \frac{m^2}{a^2} G_{mn} + \frac{n^2}{b^2} E_{mn} \right] \frac{n^2}{b^2} + \frac{m^2}{a^2} \frac{n^2}{b^2} \frac{1-\mu}{2} \right.$$

$$\left. \times \left[ c\rho_{mn} (D_{mn} - C_{mn}) + \frac{E_c}{G_{xz}} \frac{a^2}{m^2 \pi^2} c A_{mn} - G_{mn} + E_{mn} \right] \right\} = 0 \qquad (24)$$

and

$$t\delta\pi^2 \left[ \left( \frac{m^2}{a^2} G_{mn} + \frac{n^2}{b^2} E_{mn} - \frac{t}{2} \theta_{mn} C_{mn} \right) \frac{m^2}{a^2} + \frac{m^2}{a^2} \frac{n^2}{b^2} \frac{1-\mu}{2} (G_{mn} - E_{mn}) \right] + t' \delta\pi^2 \left\{ \left[ \theta_{mn} \left( \frac{c^3}{6} \right. \right. \right.$$

$$\left. + \frac{c^2 t'}{4} \right) A_{mn} + \theta_{mn} \left( \frac{c^2 + ct'}{2} \right) B_{mn} + \frac{\theta_{mn} t'}{2} C_{mn} + \frac{m^2}{a^2} \rho_{mn} c C_{mn} - \frac{E_c}{G_{xz}} \frac{c}{\pi^2} A_{mn}$$

$$\left. + \frac{n^2}{b^2} c \left(1 - \frac{1}{r}\right) D_{mn} + \frac{m^2}{a^2} G_{mn} + \frac{n^2}{b^2} E_{mn} \right] \frac{m^2}{a^2} + \frac{m^2}{a^2} \frac{n^2}{b^2} \frac{1-\mu}{2} \left[ c \rho_{mn} (C_{mn} - D_{mn}) \right.$$

$$\left. \left. - \frac{E_c}{G_{xz}} \frac{a^2}{m^2 \pi^2} c A_{mn} + G_{mn} - E_{mn} \right] \right\} = 0 \qquad (25)$$

where, in equations (20), (21), and (22), $\underline{i} \pm \underline{n}$, $\underline{m} \pm \underline{p}$, and $\underline{n} \pm \underline{q}$ are all odd.

Values of $N_o$ and $N_s$ which satisfy the linear, homogeneous set of equations (20), (21), (22), (23), (24), and (25) are called the buckling or critical loads on the panel and are noted as $N_{ocr}$ and $N_{scr}$, respectively. If all of the configuration parameters, $A_{mn}$, $B_{mn}$, $C_{mn}$, $D_{mn}$, $E_{mn}$, and $G_{mn}$ are identically equal to zero, the set of equations (20) through (25) is satisfied, but this is a trivial solution associated with the non-buckled state of the sandwich. The solution of practical interest is that which satisfies the set of equations (20) through (25) in which at least one of the configuration parameters $A_{mn}$ through $G_{mn}$ assumes a value other than zero. Such a solution can be obtained by equating to zero the determinant of the coefficients of the parameters $A_{mn}$, $B_{mn}$, $C_{mn}$, $D_{mn}$, $E_{mn}$, and $G_{mn}$ in the set of equations (20) through (25). Since there is an infinite number of equations which constitute this set, the resulting determinant is of order infinity unless $\alpha = 0$ and $N_s = 0$, in which case the determinant is of order 6.[10] For cases in which $\alpha \neq 0$ and/or $N_s \neq 0$, a satisfactory approximate solution for determining combinations of critical load can be obtained from a consideration of a finite subset from the infinite set of equations (20) through (25).

In the analogous homogeneous plate analysis by Way (see reference (10), a linear, homogeneous set consisting of 8 equations in 8 unknowns was solved. To obtain the comparable mathematical accuracy for the sandwich panel (when $W = 0$), that is to say, the comparable degree of convergence in the Rayleigh-Ritz process, necessitates the solution of a set of 48 equations in 48 unknowns from the set of equations (20) through (25). This is because 6 configuration parameters are required for each separate mode of deflection defined by the separate terms in the Fourier expansions in equations (1), (2), and (3). The reduction of this determinant of order 48 to a form usable for design presents a formidable problem.

In references (2) and (3), the further assumption that $E_c = \infty$ at this point in the analysis introduced simplifications which permitted literal reductions of the characteristic determinant. In the aforementioned references, a

---

[10] The equation which defines the buckling load for pure edgewise compression is given in equation (179) of reference (2). In the case of $E_c = \infty$, this equation reduces to equation (180) of reference (2).

characteristic determinant of order 18 was reduced to a determinant of order 3 by the expedient of adding multiples of rows and columns. The resulting determinant of order 3 was seen to be identical to the determinant of order 3 obtained in the analogous homogeneous plate analysis,[11] except that instead of a common rigidity factor $D$, there appeared a "modal rigidity" factor $D'_{mn}$ (see equation (30)). The phrase "modal rigidity" introduced here seems to describe the fact that the simply supported sandwich panel exhibits a specific rigidity corresponding to each mode defined by specific values of $m$ and $n$. Thus, a characteristic determinant of, say order 48, formed from the coefficients of $A_{mn}$, $B_{mn}$, ... , $G_{mn}$ in equations (20) through (25), may be simplified[12] to a determinant of order 8 by the simple expedient of replacing $D$ in the analogous homogeneous plate analysis by $D'_{mn}$. Therefore, the equation formed by equating to zero the determinant (of order 48) of the coefficients $A_{11}$, $A_{12}$, $A_{13}$, $A_{21}$, $A_{22}$, $A_{23}$, $A_{31}$, $A_{33}$, $B_{11}$, $B_{12}$, $B_{13}$, $B_{21}$, $B_{22}$, $B_{23}$, $B_{31}$, $B_{33}$, ... , $G_{11}$, $G_{12}$, $G_{13}$, $G_{21}$, $G_{22}$, $G_{23}$, $G_{31}$, $G_{33}$ in equations (20), (21), (22), (23), (24), and (25) can be reduced to the form[13]

---

[11] Compare equation (35) of reference (3) with the analogous solution for the homogeneous plate given in reference (9), pp. 353, 354, and 355.

[12] It is again emphasized that this simplification is based on the assumption that the transverse modulus of elasticity, $E_c$, of the core is infinite.

[13] The corresponding equation, which represents the solution of the analogous homogeneous plate problem, is given in reference (10), pp. A-134 and A-135.

$$
\begin{vmatrix}
\Omega_{11} & -\frac{1}{18}B & 0 & 0 & -\frac{4}{9}Q & 0 & 0 & 0 \\
-\frac{1}{18}B & \Omega_{12} & -\frac{3}{50}B & \frac{4}{9}Q & 0 & -\frac{4}{5}Q & 0 & 0 \\
0 & -\frac{3}{50}B & \Omega_{13} & 0 & \frac{4}{5}Q & 0 & 0 & 0 \\
0 & \frac{4}{9}Q & 0 & \Omega_{21} & -\frac{2}{9}B & 0 & 0 & 0 \\
-\frac{4}{9}Q & 0 & \frac{4}{5}Q & -\frac{2}{9}B & \Omega_{22} & -\frac{6}{25}B & \frac{4}{5}Q & -\frac{36}{25}B \\
0 & -\frac{4}{5}Q & 0 & 0 & -\frac{6}{25}B & \Omega_{23} & 0 & 0 \\
0 & 0 & 0 & 0 & \frac{4}{5}Q & 0 & \Omega_{31} & 0 \\
0 & 0 & 0 & 0 & -\frac{36}{25}B & 0 & 0 & \Omega_{33}
\end{vmatrix} = 0 \qquad (26)
$$

where

$$\Omega_{mn} = \frac{\pi^2}{32\beta}\left[\frac{\Phi_{mn}^2}{\beta^2} D'_{mn} - \frac{m^2}{\pi^2} N_{ocr}\, b^2 \left(1 - \frac{\alpha}{2}\right)\right] \qquad (27)$$

$$B = N_{ocr}\, \frac{b^2}{\pi^2}\, \frac{\alpha}{\beta} \qquad (28)$$

$$Q = N_{scr} \frac{b^2}{\pi^2} \tag{29}$$

$$D'_{mn} = \frac{E}{1-\mu^2} \left[ I_F + \frac{I_T}{1 + \frac{W}{\beta^2} \frac{\Phi^2_{mn}}{\Lambda_{mn}} + \frac{n^2 m^2 r W \left(1 - \frac{1}{r}\right)^2}{\Lambda_{mn} \left(1 + \Lambda_{mn} \frac{W}{\beta^2} r \frac{1-\mu}{2}\right)}} \right] \tag{30}$$

$$\Phi_{mn} = m^2 + n^2 \beta^2 \tag{31}$$

$$\Lambda_{mn} = m^2 + \frac{n^2 \beta^2}{r} \tag{32}$$

$$I_F = \frac{t^3 + (t')^3}{12} \tag{33}$$

$$I_T = \frac{tt'}{t + t'} \left(c + \frac{t + t'}{2}\right)^2 \tag{34}$$

$$r = \frac{G_{xz}}{G_{yz}} \tag{35}$$

$$W = \frac{ctt'}{t + t'} \frac{\pi^2}{b^2} \frac{E}{1-\mu^2} \frac{1}{G_{xz}} \tag{36}$$

and

$$\beta = \frac{a}{b} \tag{37}$$

A further assumption concerning the bending stiffness of the individual facings about their own neutral axes is now made to enable further reduction of the determinant in equation (26). This assumption is that $I_F = 0$. The division of each element of this determinant by the factor $D_T$ gives

$$\begin{vmatrix}
\Psi_{11} & k_\alpha f_1 & 0 & 0 & -\frac{4}{9}k_s & 0 & 0 & 0 \\
k_\alpha f_1 & \Psi_{12} & k_\alpha f_2 & \frac{4}{9}k_s & 0 & -\frac{4}{5}k_s & 0 & 0 \\
0 & k_\alpha f_2 & \Psi_{13} & 0 & \frac{4}{5}k_s & 0 & 0 & 0 \\
0 & \frac{4}{9}k_s & 0 & \Psi_{21} & k_\alpha f_3 & 0 & 0 & 0 \\
-\frac{4}{9}k_s & 0 & \frac{4}{5}k_s & k_\alpha f_3 & \Psi_{22} & k_\alpha f_4 & \frac{4}{5}k_s & -\frac{36}{25}k_s \\
0 & -\frac{4}{5}k_s & 0 & 0 & k_\alpha f_4 & \Psi_{23} & 0 & 0 \\
0 & 0 & 0 & 0 & \frac{4}{5}k_s & 0 & \Psi_{31} & 0 \\
0 & 0 & 0 & 0 & -\frac{36}{25}k_s & 0 & 0 & \Psi_{33}
\end{vmatrix} = 0 \tag{38}$$

where

$$\Psi_{mn} = \frac{\pi^2}{32\beta} \left[ \frac{\Phi_{mn}^2 J_{mn}}{\beta^2} - m^2 k_\alpha \left(1 - \frac{\alpha}{2}\right) \right] \tag{39}$$

$$f_1 = -\frac{1}{18} \frac{\alpha}{\beta} \tag{40}$$

$$f_2 = -\frac{3}{50} \frac{\alpha}{\beta} \tag{41}$$

$$f_3 = -\frac{2}{9} \frac{\alpha}{\beta} \tag{42}$$

$$f_4 = -\frac{6}{25} \frac{\alpha}{\beta} \tag{43}$$

$$f_5 = -\frac{1}{2} \frac{\alpha}{\beta} \tag{44}$$

$$f_6 = -\frac{27}{50} \frac{\alpha}{\beta} \tag{45}$$

$$k_\alpha = \frac{N_{ocr} b^2}{D_T \pi^2} \tag{46}$$

$$k_s = \frac{N_{scr} b^2}{D_T \pi^2} \tag{47}$$

$$D_T = \frac{EI_T}{1-\mu^2} \tag{48}$$

and

$$J_{mn} = \frac{1}{1 + \frac{W}{\beta^2}\frac{\Phi_{mn}^2}{\Lambda_{mn}} + \frac{n^2 m^2 r W \left(1 - \frac{1}{r}\right)^2}{\Lambda_{mn}\left(1 + \Lambda_{mn}\frac{W}{\beta^2}\frac{1-\mu}{2} r\right)}} \tag{49}$$

The determinant in equation (38) can be further reduced by addition of rows and columns[14] as described in the following successive operations:

$$C_5^{(2)} = C_5^{(1)} + \frac{36}{25}\frac{k_s}{\Psi_{33}} C_8^{(1)} \tag{50}$$

The resulting determinant of order 8 may be expanded by row 8, that is by $R_8^{(2)}$ leaving a determinant of order 7, which is denoted by superscript (3). Now,

$$C_5^{(4)} = C_5^{(3)} - \frac{4}{5}\frac{k_s}{\Psi_{31}} C_7^{(3)} \tag{51}$$

Expansion of this determinant of order 7 by $R_7^{(4)}$ leaves a determinant of order 6, which is denoted by superscript (5). Now,

---

[14] R signifies "row" and C signifies "column." The numerical subscript denotes the particular row or column involved. The numerical superscript denotes a specific determinant formed by adding rows and columns. Thus $R_3^{(2)}$ denotes row 3 of a second determinant formed from additions of rows and/or columns.

$$C_2^{(6)} = C_2^{(5)} + \frac{4}{5}\,\frac{k_s}{\Psi_{23}}\,C_6^{(5)}$$

and

$$C_5^{(6)} = C_5^{(5)} - \frac{k_\alpha f_4}{\Psi_{23}}\,C_6^{(5)} \qquad (52)$$

Expansion of this determinant of order 6 by $R_6^{(6)}$ leaves a determinant of order 5, which is denoted by superscript (7). Now,

$$C_2^{(8)} = C_2^{(7)} - \frac{4}{9}\,\frac{k_s}{\Psi_{21}}\,C_4^{(7)}$$

and

$$C_5^{(8)} = C_5^{(7)} - \frac{k_\alpha f_3}{\Psi_{21}}\,C_4^{(7)} \qquad (53)$$

Expansion of this determinant of order 5 by $R_4^{(8)}$ leaves a determinant of order 4, which is denoted by superscript (9). Now,

$$C_2^{(10)} = C_2^{(9)} - \frac{k_\alpha f_2}{\Psi_{13}}\,C_3^{(9)}$$

and

$$C_4^{(10)} = C_4^{(9)} - \frac{4}{5}\,\frac{k_s}{\Psi_{13}}\,C_3^{(9)} \qquad (54)$$

Expansion of this determinant of order 4 by $R_3^{(10)}$ leaves a determinant of order 3, which is denoted by superscript (11). Now,

$$C_2^{(12)} = C_2^{(11)} - \frac{k_\alpha f_1}{\Psi_{11}} C_1^{(11)}$$

and

$$C_3^{(12)} = C_3^{(11)} + \frac{4}{9} \frac{k_s}{\Psi_{11}} C_1^{(11)} \quad . \qquad (55)$$

Expansion of this determinant of order 3 by $R_2^{(12)}$ leaves a determinant of order 2. Thus, equation (38) can now be written as follows:

$$\left[\Psi_{12} - \left(\frac{16}{25\Psi_{23}} + \frac{16}{81\Psi_{21}}\right) k_s^2 - \left(\frac{f_2^{2'}}{\Psi_{13}} + \frac{f_1^2}{\Psi_{11}}\right) k_\alpha^2\right]\left[\Psi_{22} - \left(\frac{1296}{625\Psi_{33}}\right.\right.$$

$$\left.\left. + \frac{16}{25\Psi_{31}} + \frac{16}{25\Psi_{13}} + \frac{16}{81\Psi_{11}}\right) k_s^2 - \left(\frac{f_4^2}{\Psi_{23}} + \frac{f_3^2}{\Psi_{21}}\right) k_\alpha^2\right]$$

$$- k_\alpha^2 k_s^2 \left[\frac{4}{5}\frac{f_4}{\Psi_{23}} - \frac{4}{5}\frac{f_2}{\Psi_{13}} - \frac{4}{9}\frac{f_3}{\Psi_{21}} + \frac{4}{9}\frac{f_1}{\Psi_{11}}\right]^2 = 0 \quad . \qquad (56)$$

Equation (56) was used to obtain the data from which the design curves (figs. 6 to 32 inclusive) were constructed.

## Results and Discussion

The magnitudes of arbitrary combinations of edgewise bending, compression, and shear loads which will cause a simply supported rectangular sandwich panel to buckle may be found from numerical solution of the following equation:

$$\begin{vmatrix} P_{1,1} & P_{1,2} & \cdots & P_{1,\infty} \\ P_{2,1} & P_{2,2} & \cdots & P_{2,\infty} \\ \cdot & & & \\ \cdot & & & \\ \cdot & & & \\ P_{\infty,1} & P_{\infty,2} & \cdots & P_{\infty,\infty} \end{vmatrix} = 0 \qquad (57)$$

where the elements $P_{p,q}$ are the coefficients of the configuration parameters $A_{mn}$, $B_{mn}$, ... , $G_{mn}$ in equations (20), (21), (22), (23), (24), and (25).

An approximation to the buckling criteria can be obtained from consideration of a minor of finite order from the determinant of infinite order in equation (57). Since the problem at hand involves a layered system in which 6 parameters are necessary to satisfy the equilibrium equations for each specific mode of panel configuration (each value of m and/or n in equations (20) through (25) defines a separate mode), the approximating determinant (minor of determinant in equation (57)) must be selected in multiples of 6. Thus, a first approximation[15] can be obtained by equating to zero the determinant of order 6 with elements formed from the coefficients of $A_{11}$, $B_{11}$, ... , $G_{11}$ in equations (20) through (25). A second (more accurate) approximation can be obtained by equating to zero the determinant of order 24 with elements formed from the coefficients of $A_{11}$, $B_{11}$, ... , $G_{11}$, $A_{12}$, $B_{12}$, ... , $G_{12}$, $A_{21}$, $B_{21}$, ... , $G_{21}$, and $A_{22}$, $B_{22}$, ... , $G_{22}$. A third approximation (still more accurate) can be obtained by equating to zero the determinant of order 54 with elements formed from the coefficients of $A_{11}$, $B_{11}$, ... , $G_{11}$, $A_{12}$, $B_{12}$, ... , $G_{12}$, $A_{13}$, $B_{13}$, ... , $G_{13}$, $A_{21}$, $B_{21}$, ... , $G_{21}$, $A_{22}$, $B_{22}$, ... , $G_{22}$, $A_{23}$, $B_{23}$, ... , $G_{23}$, $A_{31}$, $B_{31}$, ... , $G_{31}$, $A_{32}$, $B_{32}$, ... , $G_{32}$,

[15] This approximation is equation (179) of reference (2). Note that equation (179) of reference (2) is exact for pure edgewise compression. For other more general types of loading, this approximation will often be far in error.

and $A_{33}$, $B_{33}$, . . . , $G_{33}$. The accuracy of any approximation can be estimated by determining a result from a larger determinant following the scheme of order of approximation discussed above.

The assumption that the transverse modulus of elasticity of the core is infinite,[16] that is, $E_c = \infty$, introduces welcome simplifications in equation (57) and in all approximate forms of equation (57). In the case of $E_c = \infty$, the equation formed from the "third approximation" referred to above is as follows:

$$\begin{vmatrix}
\Omega_{11} & -\frac{1}{18}B & 0 & 0 & -\frac{4}{9}Q & 0 & 0 & 0 & 0 \\
-\frac{1}{18}B & \Omega_{12} & -\frac{3}{50}B & \frac{4}{9}Q & 0 & -\frac{4}{5}Q & 0 & 0 & 0 \\
0 & -\frac{3}{50}B & \Omega_{13} & 0 & \frac{4}{5}Q & 0 & 0 & 0 & 0 \\
0 & \frac{4}{9}Q & 0 & \Omega_{21} & -\frac{2}{9}B & 0 & 0 & -\frac{4}{5}Q & 0 \\
-\frac{4}{9}Q & 0 & \frac{4}{5}Q & -\frac{2}{9}B & \Omega_{22} & -\frac{6}{25}B & \frac{4}{5}Q & 0 & -\frac{36}{25}B \\
0 & -\frac{4}{5}Q & 0 & 0 & -\frac{6}{25}B & \Omega_{23} & 0 & \frac{36}{25}Q & 0 \\
0 & 0 & 0 & 0 & \frac{4}{5}Q & 0 & \Omega_{31} & -\frac{1}{2}B & 0 \\
0 & 0 & 0 & -\frac{4}{5}Q & 0 & \frac{36}{25}Q & -\frac{1}{2}B & \Omega_{32} & -\frac{27}{50}B \\
0 & 0 & 0 & 0 & -\frac{36}{25}B & 0 & 0 & -\frac{27}{50}B & \Omega_{33}
\end{vmatrix} = 0 \qquad (58)$$

[16] See page 77 of reference (2).

where $\Omega_{mn}$, $B$, and $Q$ are defined in equations (27), (28), and (29).

The assumed configuration involved in this approximation is sufficiently "flexible" to assure convergence adequate for design purposes for certain values of $\frac{a}{b}$ and $W$. To obtain more accurate approximations (for any values of $\frac{a}{b}$ and $W$) to the buckling loads, and hence to estimate the accuracy of any given calculation, requires consideration of a larger number of equations from the infinite number given in equations (20) through (25). When the load on the panel is primarily bending, the accuracy of any approximation can be estimated from a comparison with the values for critical load obtained for pure edgewise bending in reference (2), figure 6, and reference (3), figures 4, 5, and 6. When the load on the panel is primarily shear, the accuracy in any approximation often cannot be estimated so readily. However, for panels with isotropic cores ($r$ = 1.0), accuracy can be estimated for edgewise loading which is primarily shear from results obtained in reference (4).

The numerical results presented as design curves in this report were obtained from a modified form of equation (58). Specifically, the configuration defined by $m$ = 3 and $n$ = 2 was deleted from equation (58) to give equation (26). The assumption that the bending rigidities of the individual facings about their own middle planes is negligible permits equation (26) to be simplified[17] to equation (56). Equation (56) was used to prepare all design curves in this paper. For $r$ = 1.0, the curves are independent of Poisson's ratio, $\mu$, of the facings. In the curves for $r$ = 0.4 and for $r$ = 2.5, $\mu$ was taken equal to 1/3.[18] The results of several comparison calculations made for both $\mu$ = 1/4 and for $\mu$ = 1/3 produced no discernible differences in the design curves. Some of the design curves are shown as solid lines and others are shown as dashed lines. The solid lines indicate computed data that are estimated to be accurate to within 10 percent of the limit value that could be approached by using additional equations and configuration parameters. The dashed lines indicate computed data that are estimated to be more than 10 percent too high with respect to limit values. These estimates are based on studies of the more accurate data in references (2) and (3) for the critical load associated with

---

[17] Details of this simplification are given in the section entitled Mathematical Analysis.

[18] $\mu$ = 1/3 was used for computation of numerical results in references (3) and (5) when $r \neq 1.0$.

pure edgewise bending and in reference (4) for the critical load associated with pure edgewise shear. Convergence of the numerical results is best when $\beta$ does not vary significantly from unity and when $W$ is small. For example, the convergence accuracy of the results for the square panel $\beta = 1$, $r = 2.5$, and $W \leqq 0.150$ is believed closer than 2 percent. An idea of the behavior of the convergence can be obtained by studying the pattern of solid to dashed lines that occurs in figures 5 to 32 inclusive. The dashed lines, which represent data with convergence accuracy of less than 10 percent, are presented for two reasons. First, these data will be of interest to the analyst who wishes to compare with results obtained from consideration of a larger number of configuration parameters, and who is thus able to estimate rapidity of convergence. Second, in the absence of better results, these data are believed to be of practical use to the designer. The designer is perhaps aided by the knowledge that convergence errors always cause the prediction of critical load to be too high.

Excellent discussions of convergence in the Rayleigh-Ritz process as applied to analyses of homogeneous plates are presented in references 1, 6, 7, 8, and 9.

## Use of Design Curves

The design curves in this paper are presented by means of interaction curves, that is, curves that can be used to obtain the value of $N_{ocr}$ [19] (the maximum value of the unit loading on the panel associated with edgewise bending) required to produce buckling when a given value of $N_{scr}$ [20] (the maximum value of the unit loading on the panel associated with edgewise shear) is also present.

The notation used with the design curves is presented in figure 5.

---

[19] The edgewise buckling moment, $M_{ocr}$, corresponding to $N_{ocr}$ may be computed from the equation

$$M_{ocr} = N_{ocr} \frac{b^2}{6} .$$

[20] The edgewise shear force on a panel edge may be computed by multiplying $N_{scr}$ by the length of panel edge.

First, calculate the ratio, $\underline{\beta} = \frac{a}{b}$, of the panel. The curves in this report are for use with panel ratios

$$0.4 \leq \beta \leq 2.0 \quad .$$

Calculate the ratio, $\underline{r} = \frac{G_{xz}}{G_{yz}}$ .

Select the proper curve sheet that corresponds to the closest values of $\beta$ and $r$. Now, calculate the value of $W$ from the equation

$$W = \frac{ctt'}{t + t'} \frac{\pi^2}{b^2} \frac{E}{1-\mu^2} \frac{1}{G_{xz}} \quad .$$

On the curve sheet that has been selected, identify which one of the family of curves most closely corresponds to the value of $W$ that has just been computed. This curve will now provide numerical values of critical load factors from which buckling loads may be found. Thus, if a designer knows the magnitude of edgewise bending which a panel must carry, he may calculate the buckling factor $k_2$ from the equation

$$k_2 = \frac{b^2}{\pi^2 D_T} N_{ocr}$$

where $N_{ocr}$ may be obtained from the edgewise moment, $M_{ocr}$, by the equation

$$N_{ocr} = \frac{6}{b^2} M_{ocr} \quad .$$

Knowing the factor, $k_2$, it is possible to determine the factor $k_s$ from the curve previously selected. The value of the unit edgewise shear load, $N_{scr}$, which together with the value of $N_{ocr}$ will cause the panel to

buckle, may now be calculated from the equation

$$N_{scr} = \frac{\pi^2 D_T}{b^2} k_{scr}$$

The curves are believed to be prepared in such a manner as to facilitate interpolative procedures that will occur to the designer.

## Literature Cited


(1) Batdorf, S. B., and Stein, M.
1947. Critical Combinations of Shear and Direct Stress for Simply Supported Rectangular Flat Plates, NACA TN 1223.

(2) Kimel, W. R.
1956. Elastic Buckling of a Simply Supported Rectangular Sandwich Panel Subjected to Combined Edgewise Bending and Compression, Forest Products Laboratory Rept. No. 1857.

(3) _____
1956. Supplement to Elastic Buckling of a Simply Supported Rectangular Sandwich Panel Subjected to Combined Edgewise Bending and Compression. Results for Panels with Facings of Either Equal or Unequal Thickness and With Orthotropic Cores, Forest Products Laboratory Rept. No. 1857-A.

(4) Kuenzi, E. W., and Ericksen, W. S.
1951. Shear Stability of Flat Panels of Sandwich Construction, Forest Products Laboratory Rept. No. 1560.

(5) Norris, Charles B.
1956. Compressive Buckling Design Curves for Sandwich Panels With Isotropic Facings and Orthotropic Cores. Forest Products Laboratory Rept. No. 1854, 5 pp., illus.

(6) Seydel, E.
1933. Uber das Ausbeulen von rechteckigen, isotropen oder orthogonal-anisotropen Platten bei Schubbeanspruchung, Ingenieur-Archiv. IV. Band.

(7) Smith, R. C. T.
1946. The Buckling of Plywood Plates in Shear, A.C.A. Report ACA 29, October.

(8) Stein, Manuel, and Neff, John
1947. Buckling Stresses of Simply Supported Rectangular Flat Plates in Shear, NACA TN 1222.

(9) Timoshenko, S.
1936. Theory of Elastic Stability, First edition, New York.

(10) Way, Stewart
1936. Stability of Rectangular Plates Under Shear and Bending Forces, Journal of Applied Mechanics, Vol. 3, No. 4, December, pp. A-131 to A-135.

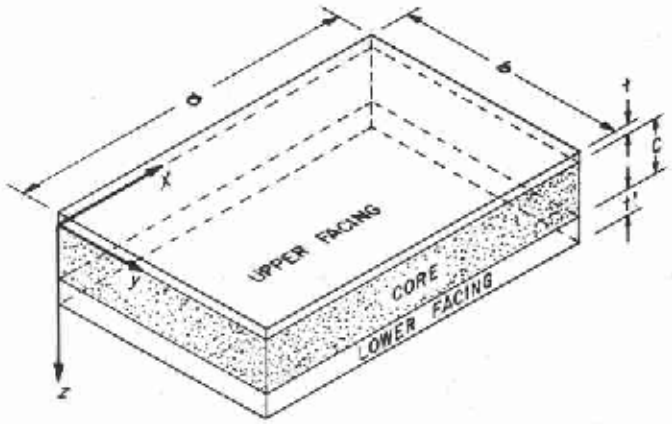


M 108 739

Figure 1. --Isometric drawing of a sandwich panel.

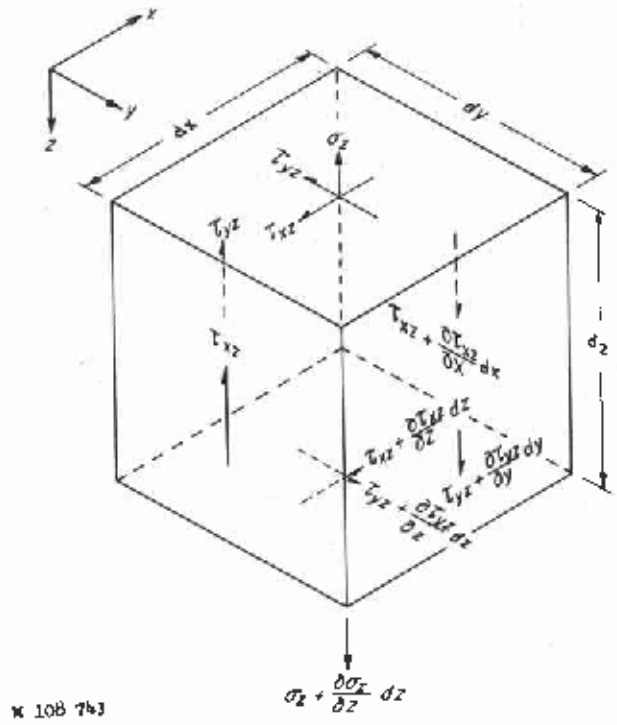


M 108 743

Figure 2. --Differential element of the core.

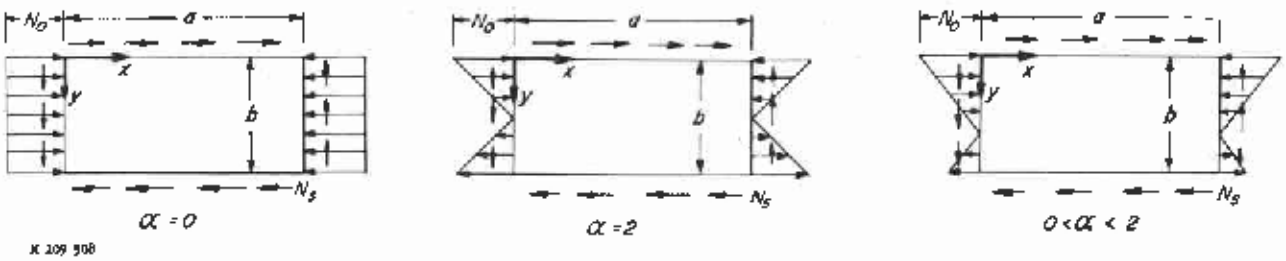


M 109 308

Figure 3. --Top view of sandwich panel showing different combinations of edgewise bending and compression as defined by $\alpha$. $N_o$ is normal edge load per unit width, b, of panel. $N_s$ is shear edge load per unit length of edges, a and b, of panel.

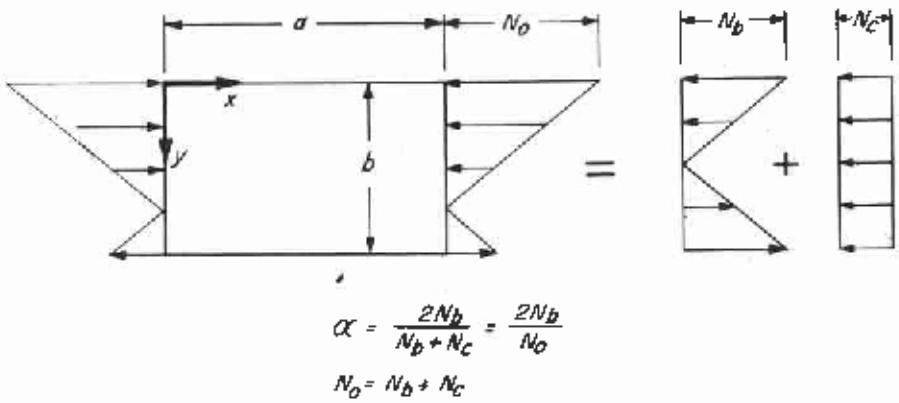


M 109 309

Figure 4. --Pictorialized definition of $\alpha$, $N_o$, $N_b$, and $N_c$.

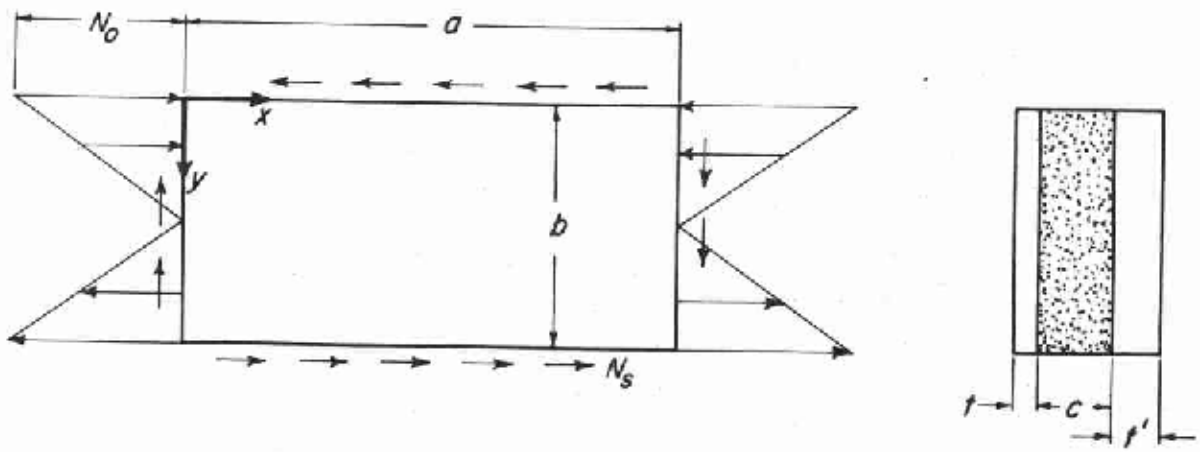


$$N_{ocr} = \frac{\pi^2 D_T}{b^2} k_2 \quad , \quad N_{scr} = \frac{\pi^2 D_T}{b^2} k_s$$

$$W = \frac{ctt'}{t+t'} \frac{\pi^2}{b^2} \frac{E}{1-\mu^2} \frac{1}{G_{xz}} = 0$$

$$\beta = \frac{a}{b}$$

M 109 307

Figure 5. --Drawing of sandwich panel including notations and formulas used with design curves presented in figures 6 to 32.

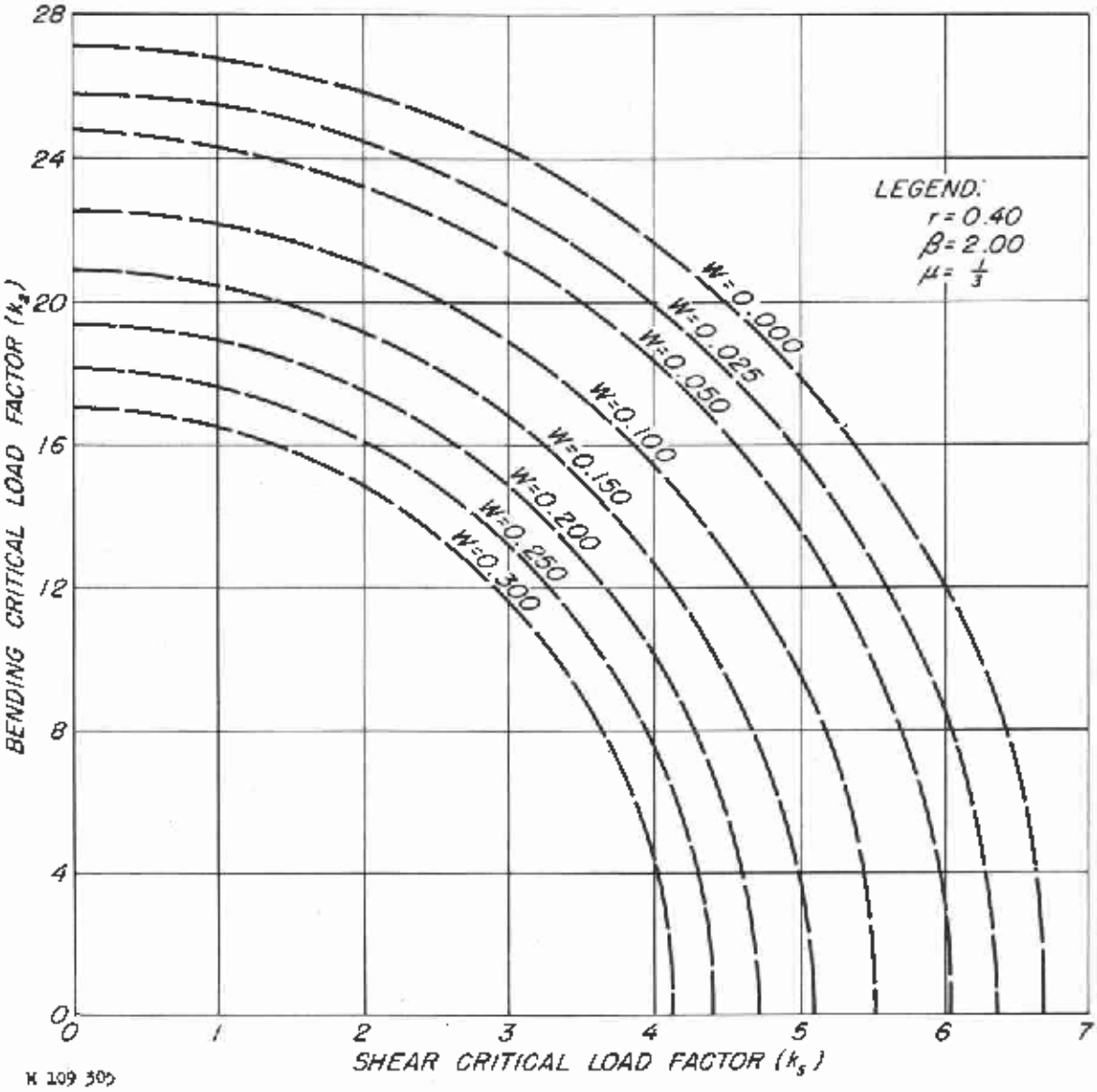


Figure 6. --Critical load factor $k_z$ versus critical load factor $k_s$ for $r = 0.40$, $\beta = 2.00$, and $0.00 \leqq \overline{W} \leqq 0.300$. See figure 5 for notation. Dashed lines indicate computed results which are too high by more than 10 percent because of convergence behavior.

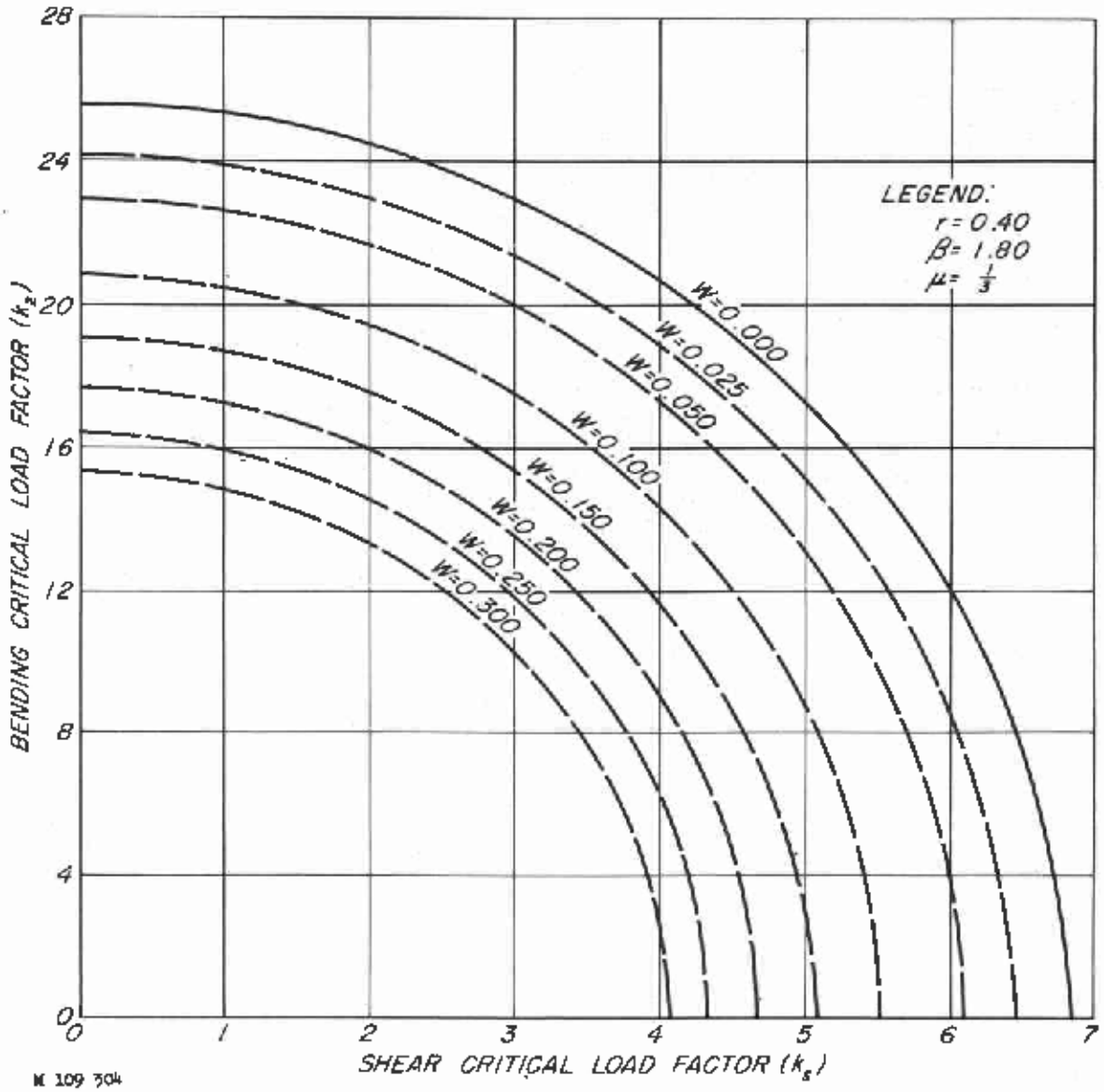


Figure 7. --Critical load factor $k_2$ versus critical load factor $k_s$ for $r = 0.40$, $\beta = 1.80$, and $0.00 \leq W \leq 0.300$. See figure 5 for notation. Dashed lines indicate computed results which are too high by more than 10 percent because of convergence behavior.

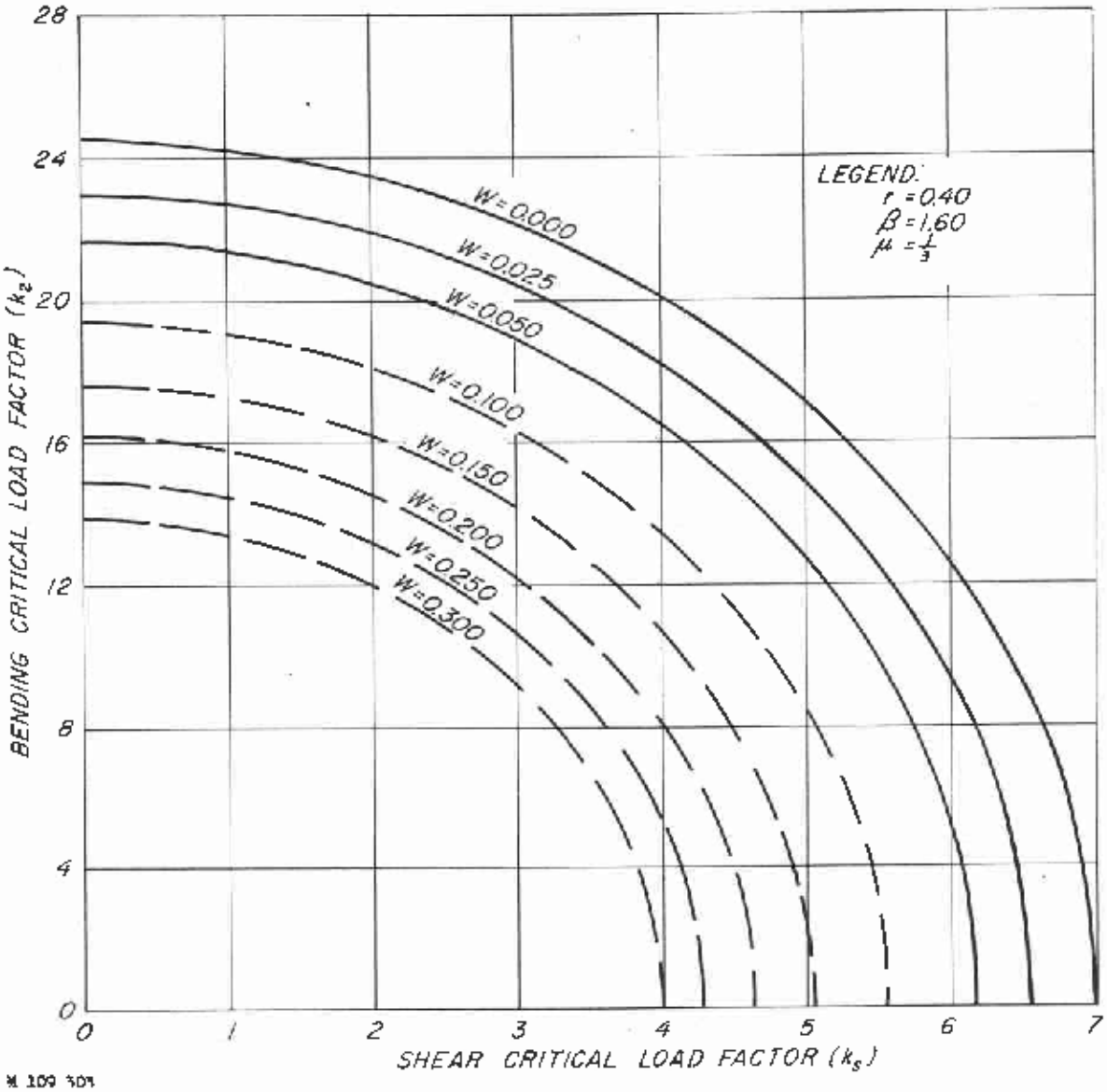


Figure 8. --Critical load factor $k_2$ versus critical load factor $k_s$ for $r = 0.40$, $\beta = 1.60$, and $0.00 \leqq W \leqq 0.300$. See figure 5 for notation. Dashed lines indicate computed results which are too high by more than 10 percent because of convergence behavior.



GPO 828868 • 5

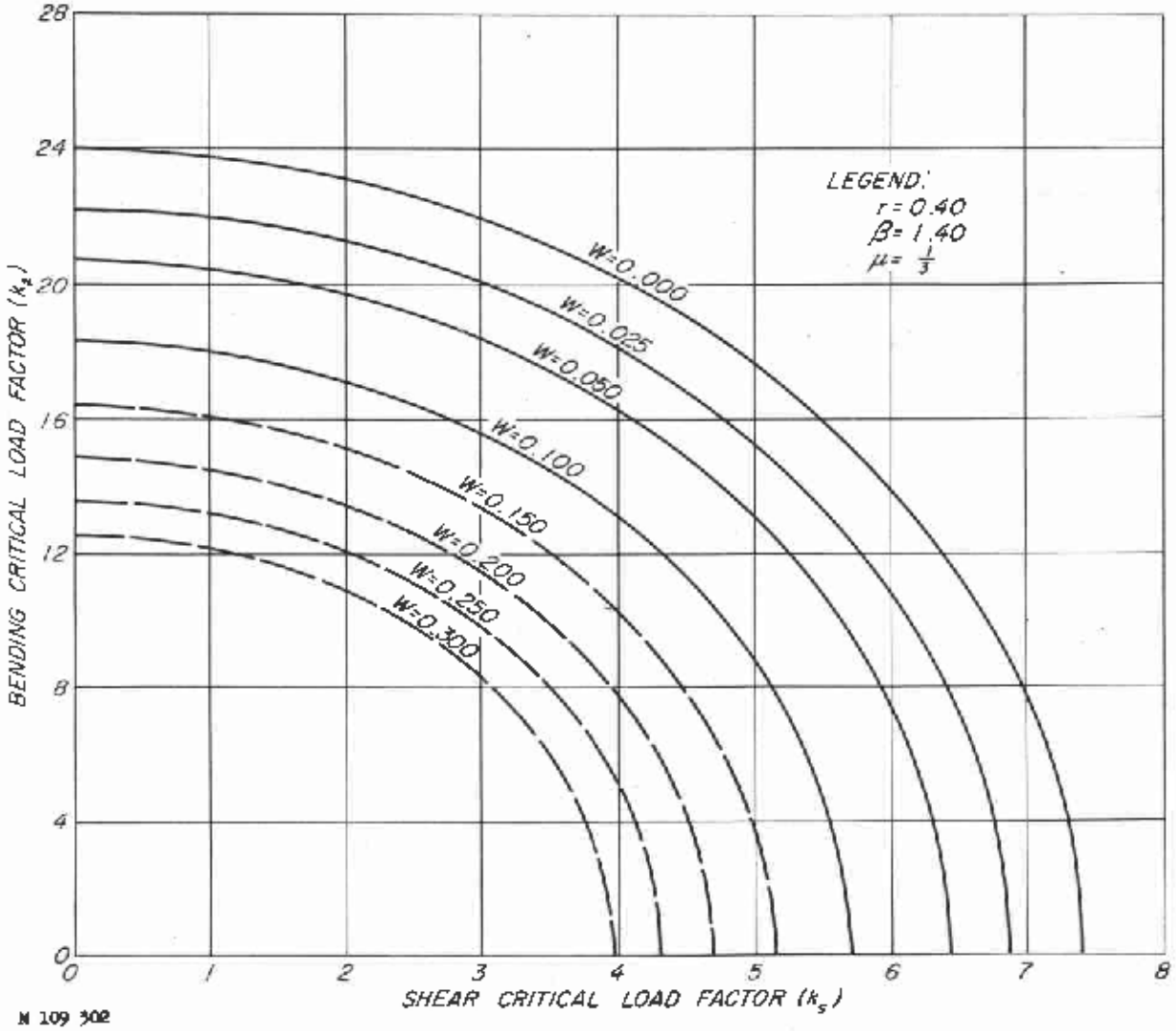


Figure 9. --Critical load factor $k_z$ versus critical load factor $k_s$ for $r = 0.40$, $\beta = 1.40$, and $0.00 \leq W \leq 0.300$. See figure 5 for notation. Dashed lines indicate computed results which are too high by more than 10 percent because of convergence behavior.

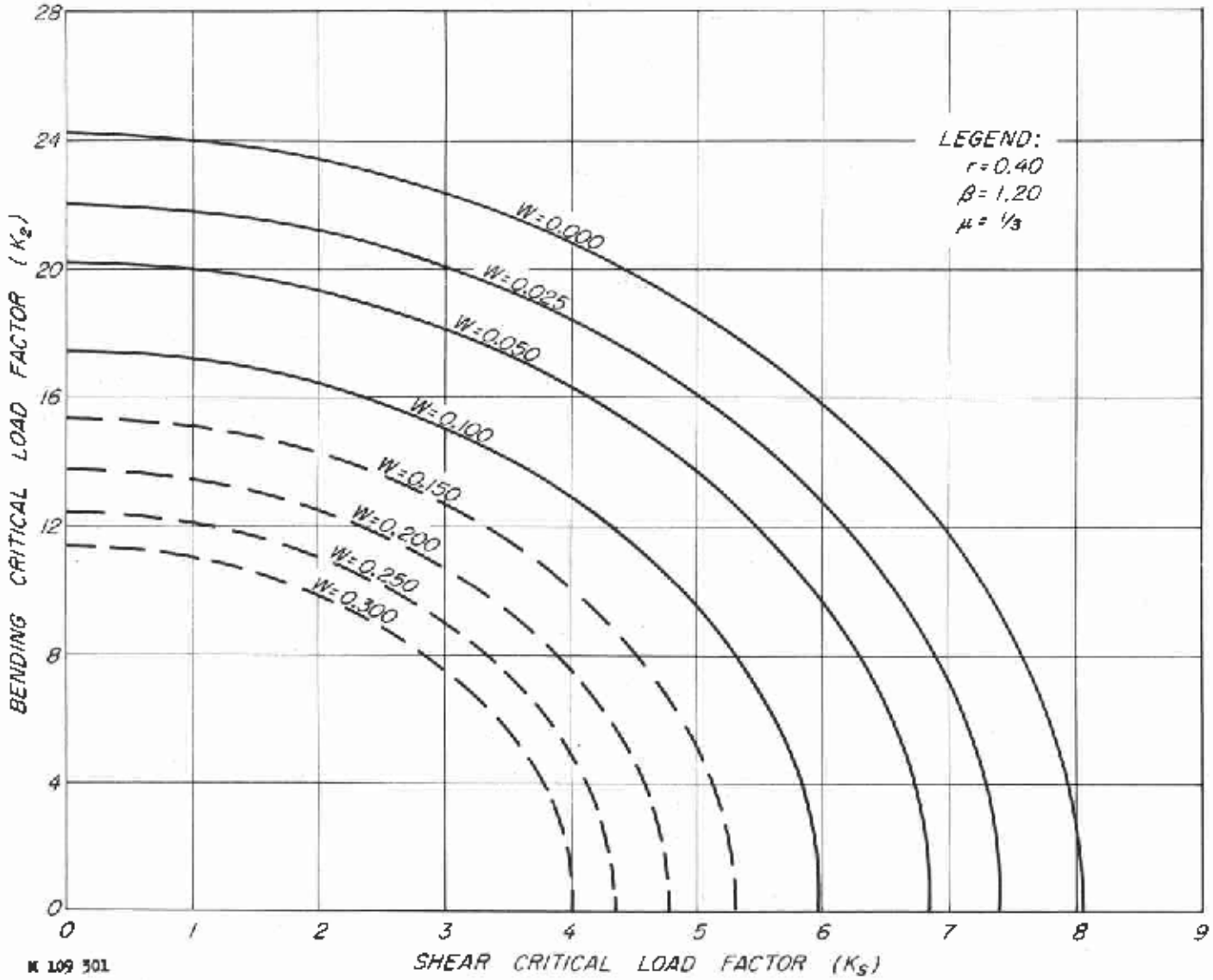


Figure 10. --Critical load factor $k_2$ versus critical load factor $k_s$ for $r$ = 0.40, $\beta$ = 1.20, and $0.00 \leq W \leq 0.300$. See figure 5 for notation. Dashed lines indicate computed results which are too high by more than 10 percent because of convergence behavior.

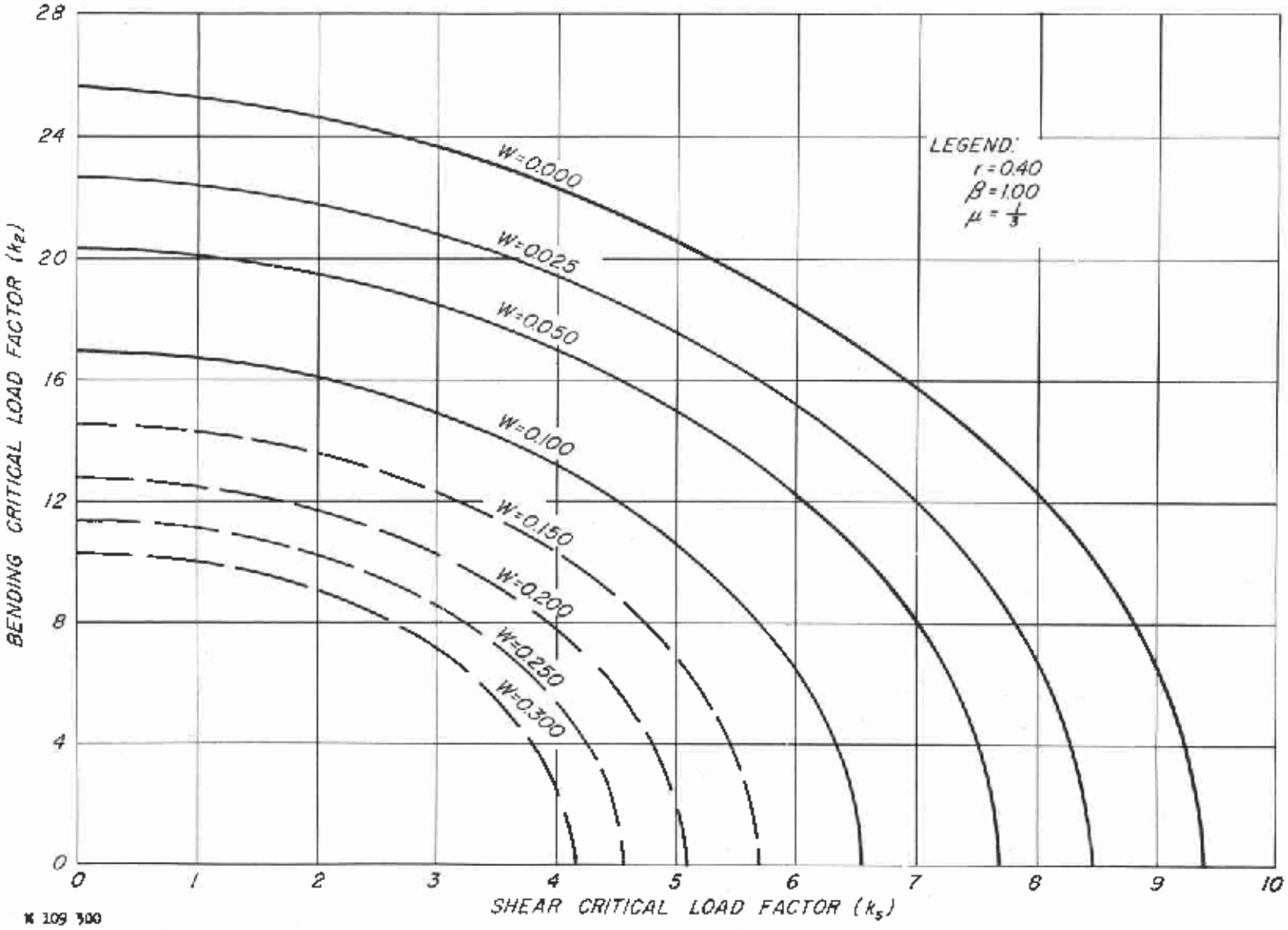


Figure 11. --Critical load factor $k_2$ versus critical load factor $k_s$ for $r = 0.40$, $\beta = 1.00$, and $0.00 \leqq W \leqq 0.300$. See figure 5 for notation. Dashed lines indicate computed results which are too high by more than 10 percent because of convergence behavior.

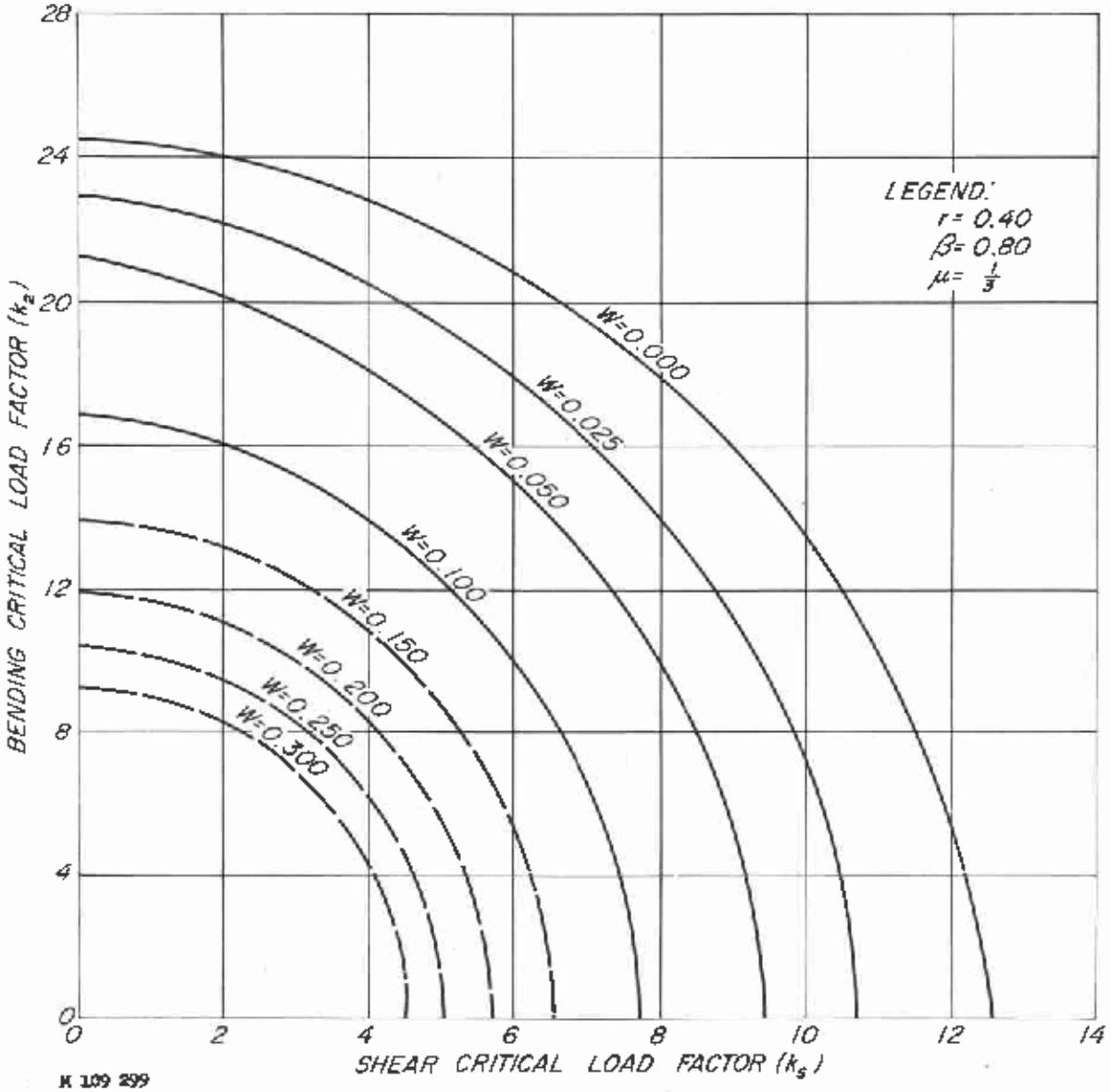


Figure 12. --Critical load factor $\underline{k_2}$ versus critical load factor $\underline{k_s}$ for $\underline{r}$ = 0.40, $\underline{\beta}$ = 0.80, and $0.00 \leq \underline{W} \leq 0.300$. See figure 5 for notation. Dashed lines indicate computed results which are too high by more than 10 percent because of convergence behavior.

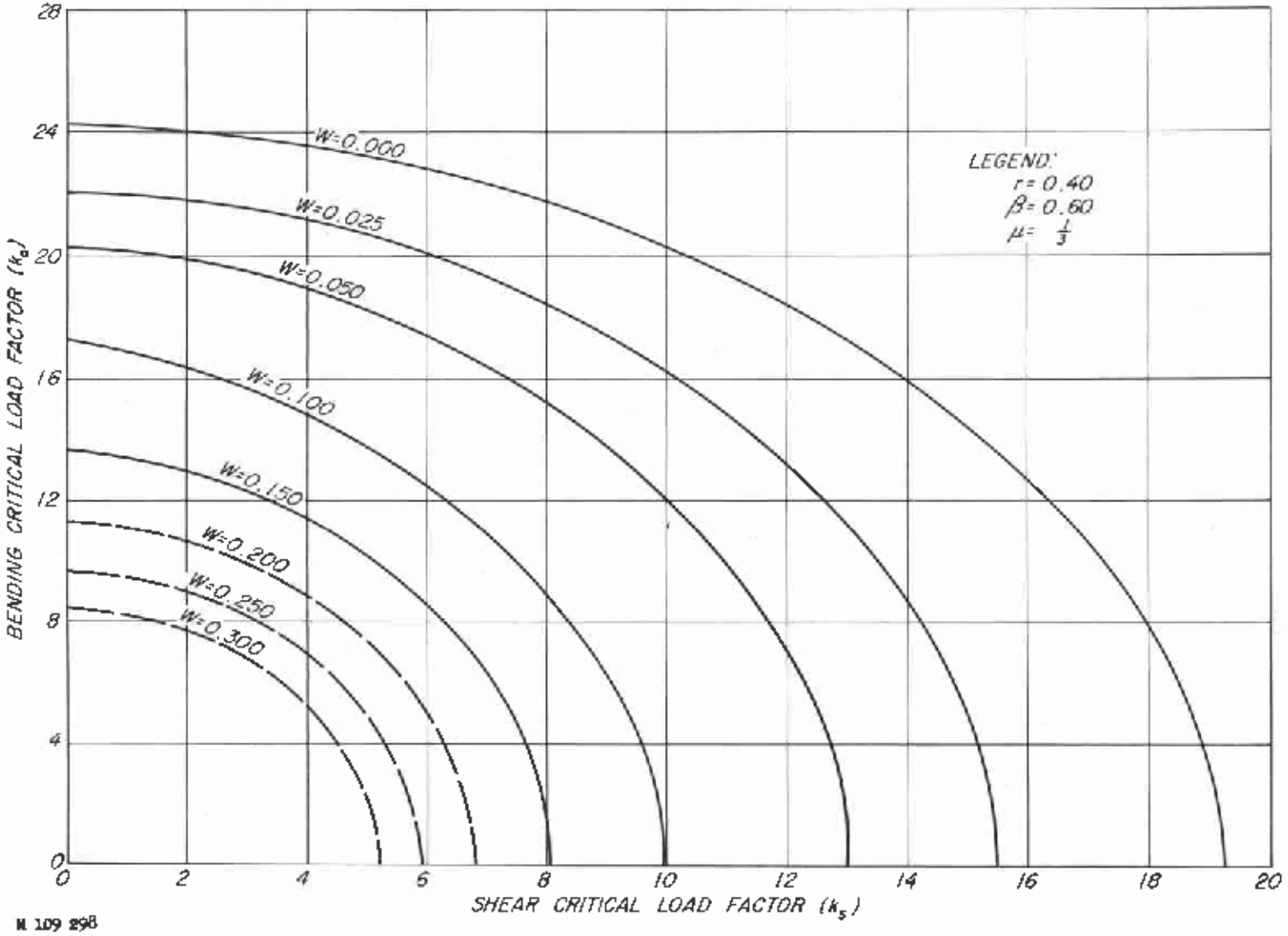


Figure 13. --Critical load factor $k_2$ versus critical load factor $k_s$ for $r = 0.40$, $\beta = 0.60$, and $0.00 \leqq W \leqq 0.300$. See figure 5 for notation. Dashed lines indicate computed results which are too high by more than 10 percent because of convergence behavior.

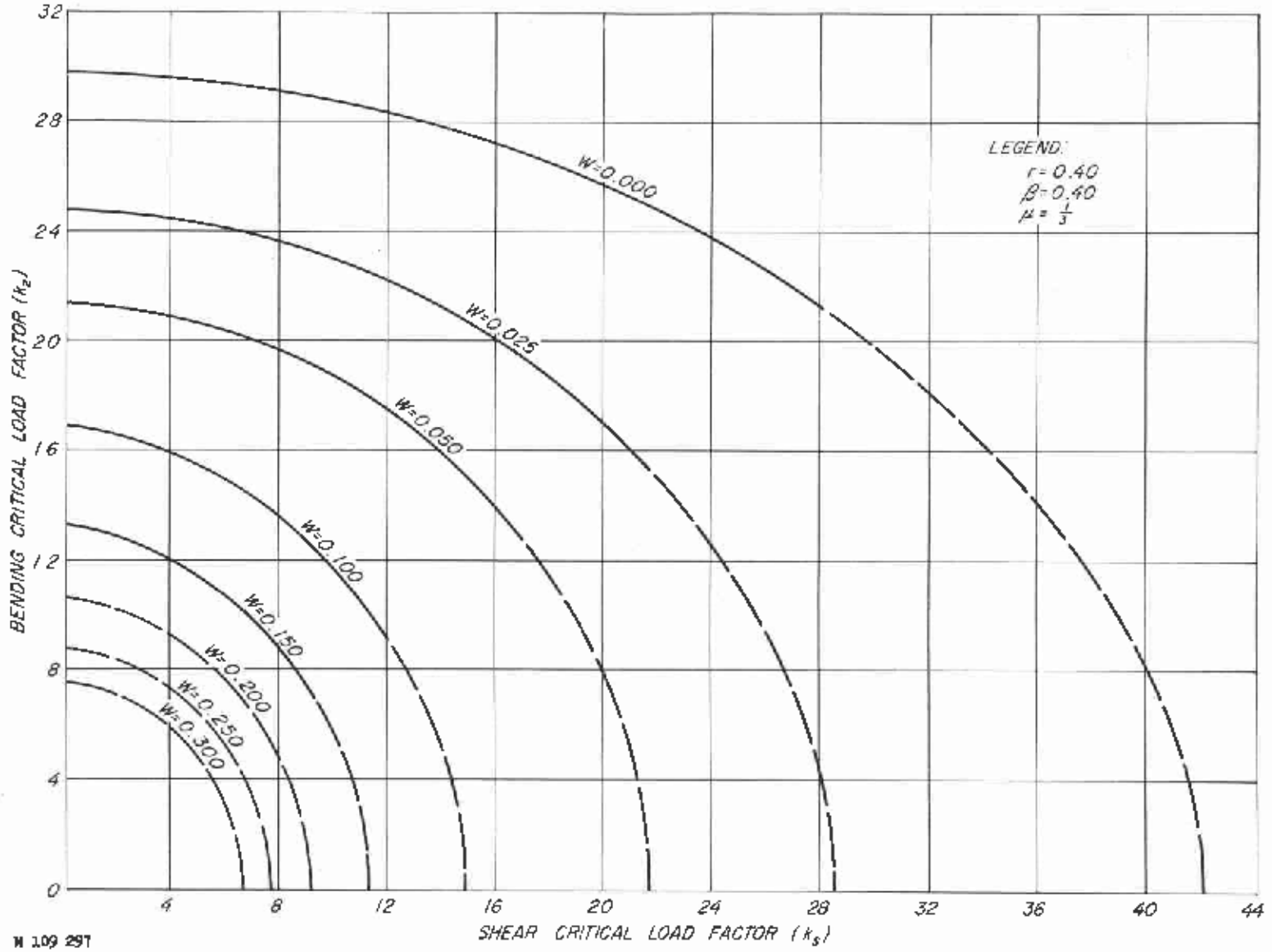


Figure 14. --Critical load factor $k_2$ versus critical load factor $k_s$ for $r = 0.40$, $\beta = 0.40$, and $0.00 \leq W \leq 0.300$. See figure 5 for notation. Dashed lines indicate computed results which are too high by more than 10 percent because of convergence behavior.

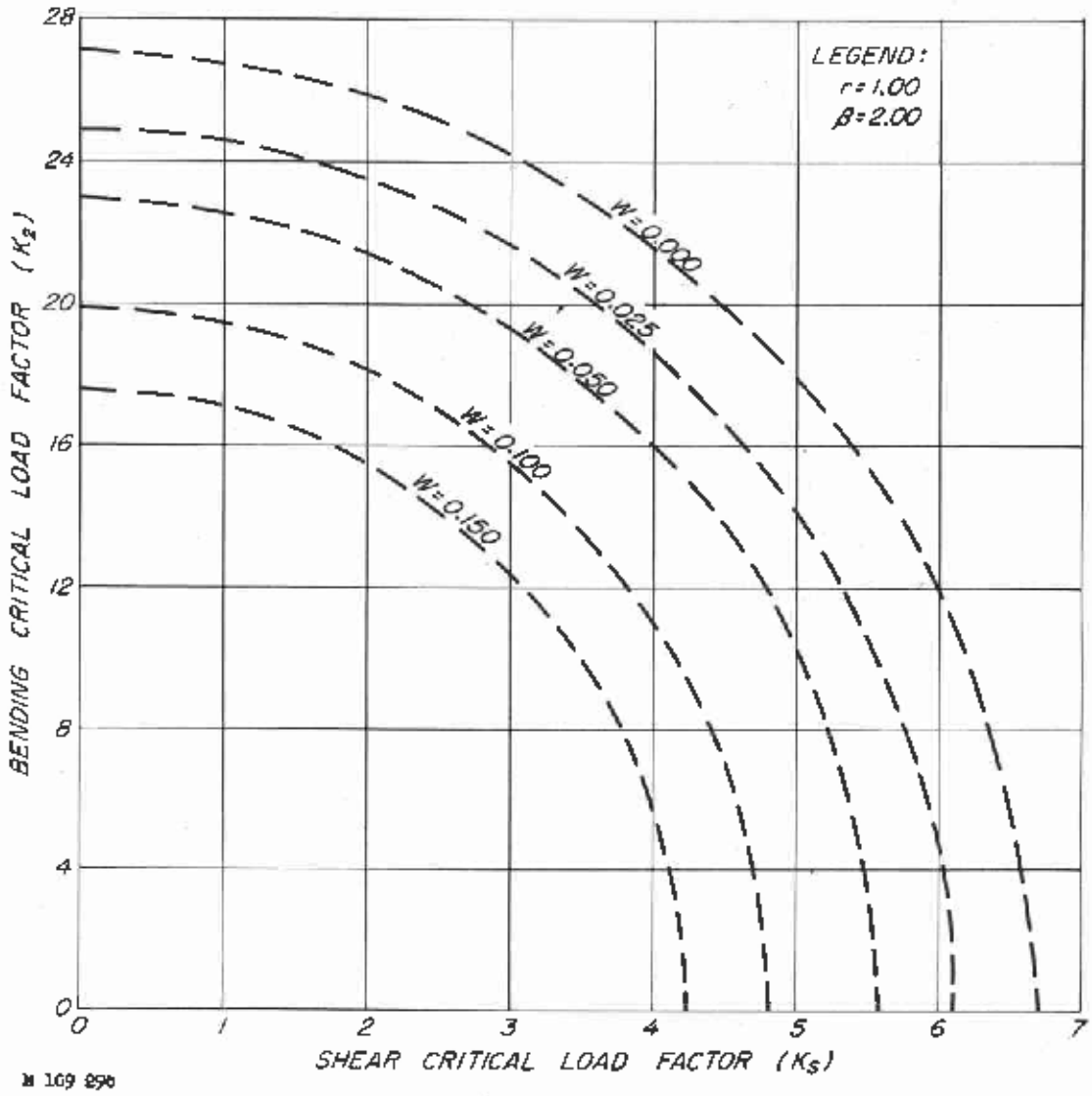


Figure 15. --Critical load factor $k_2$ versus critical load factor $k_s$ for $r = 1.00$, $\beta = 2.00$, and $0.00 \leqq W \leqq 0.150$. See figure 5 for notation. Dashed lines indicate computed results which are too high by more than 10 percent because of convergence behavior.

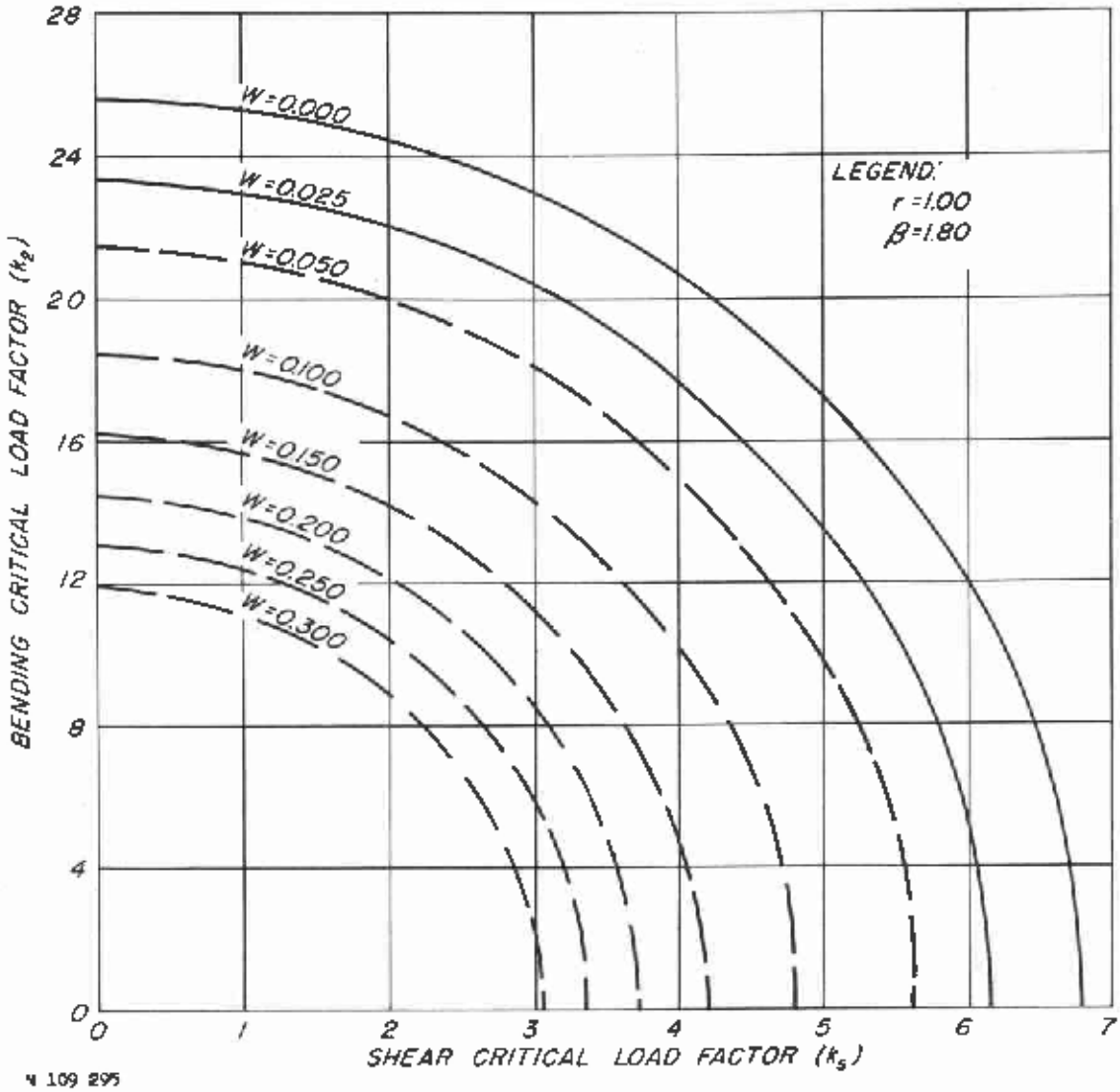


Figure 16. --Critical load factor $k_z$ versus critical load factor $k_s$ for $r = 1.00$, $\beta = 1.80$, and $0.00 \leq \overline{W} \leq 0.300$. See figure 5 for notation. Dashed lines indicate computed results which are too high by more than 10 percent because of convergence behavior.



GPO 825868 - 4

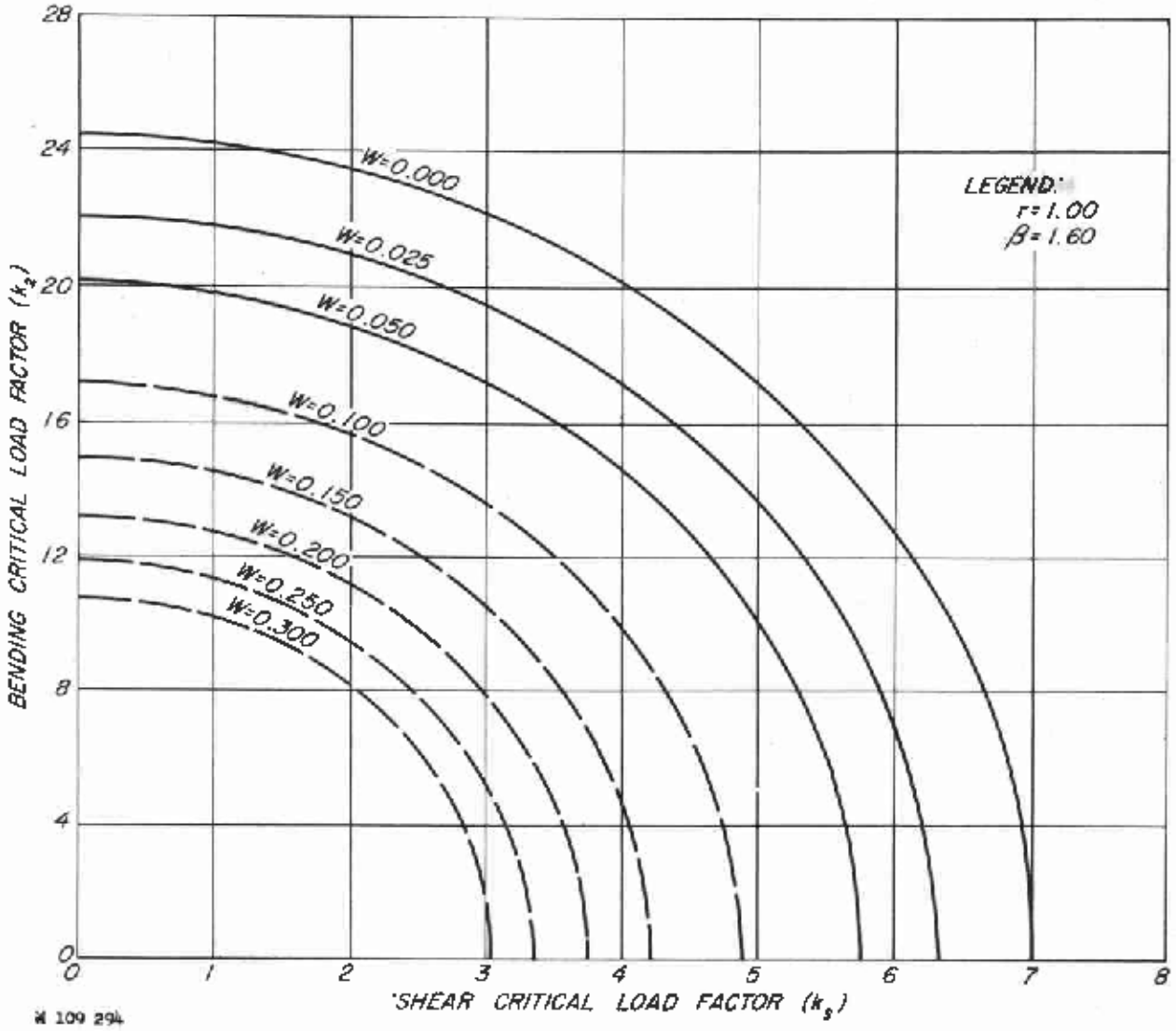


Figure 17. --Critical load factor $k_2$ versus critical load factor $k_s$ for $r = 1.00$, $\beta = 1.60$, and $0.00 \leq W \leq 0.300$. See figure 5 for notation. Dashed lines indicate computed results which are too high by more than 10 percent because of convergence behavior.

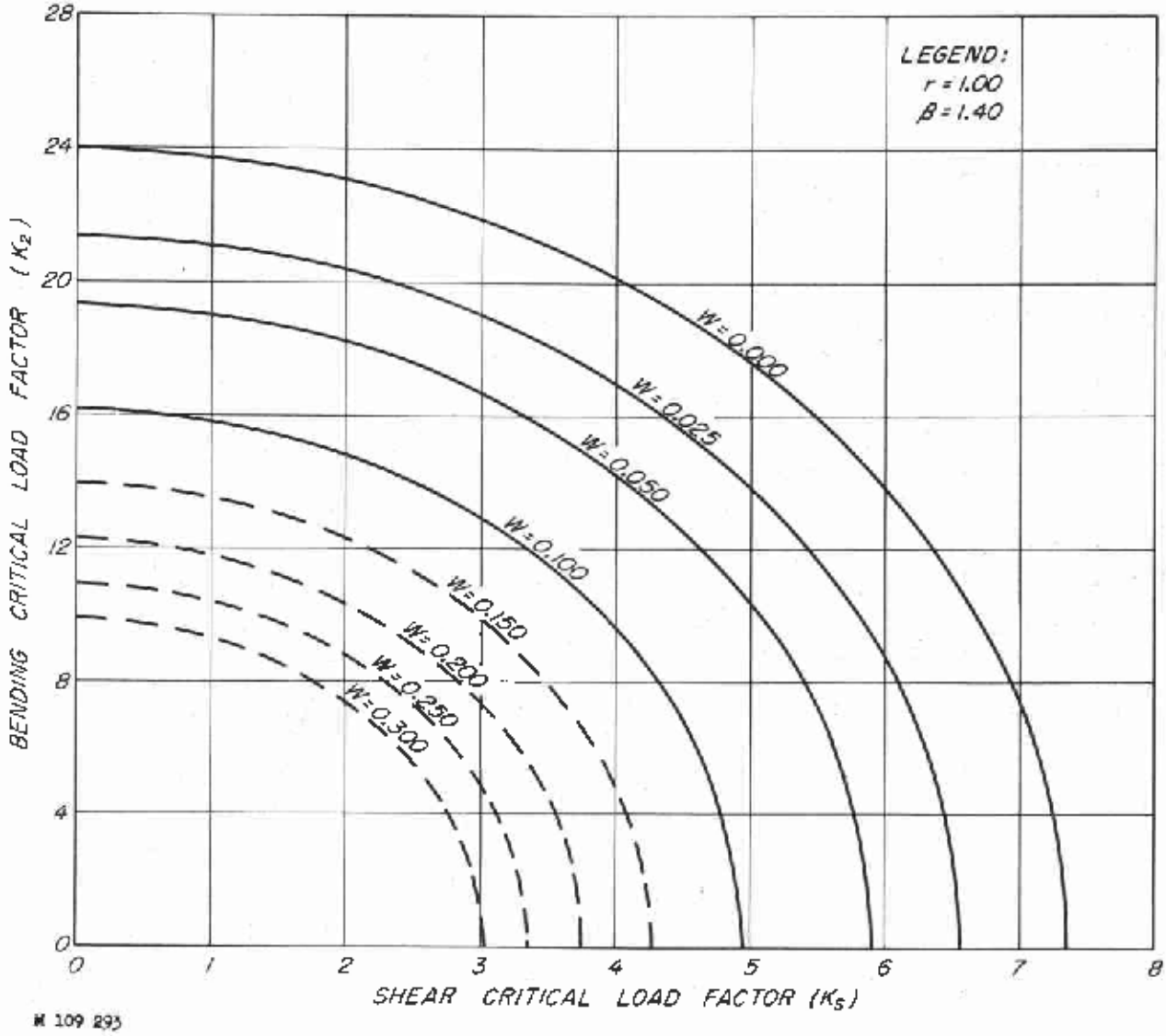


Figure 18. --Critical load factor $k_2$ versus critical load factor $k_s$ for $r = 1.00$, $\beta = 1.40$, and $0.00 \leq W \leq 0.300$. See figure 5 for notation. Dashed lines indicate computed results which are too high by more than 10 percent because of convergence behavior.

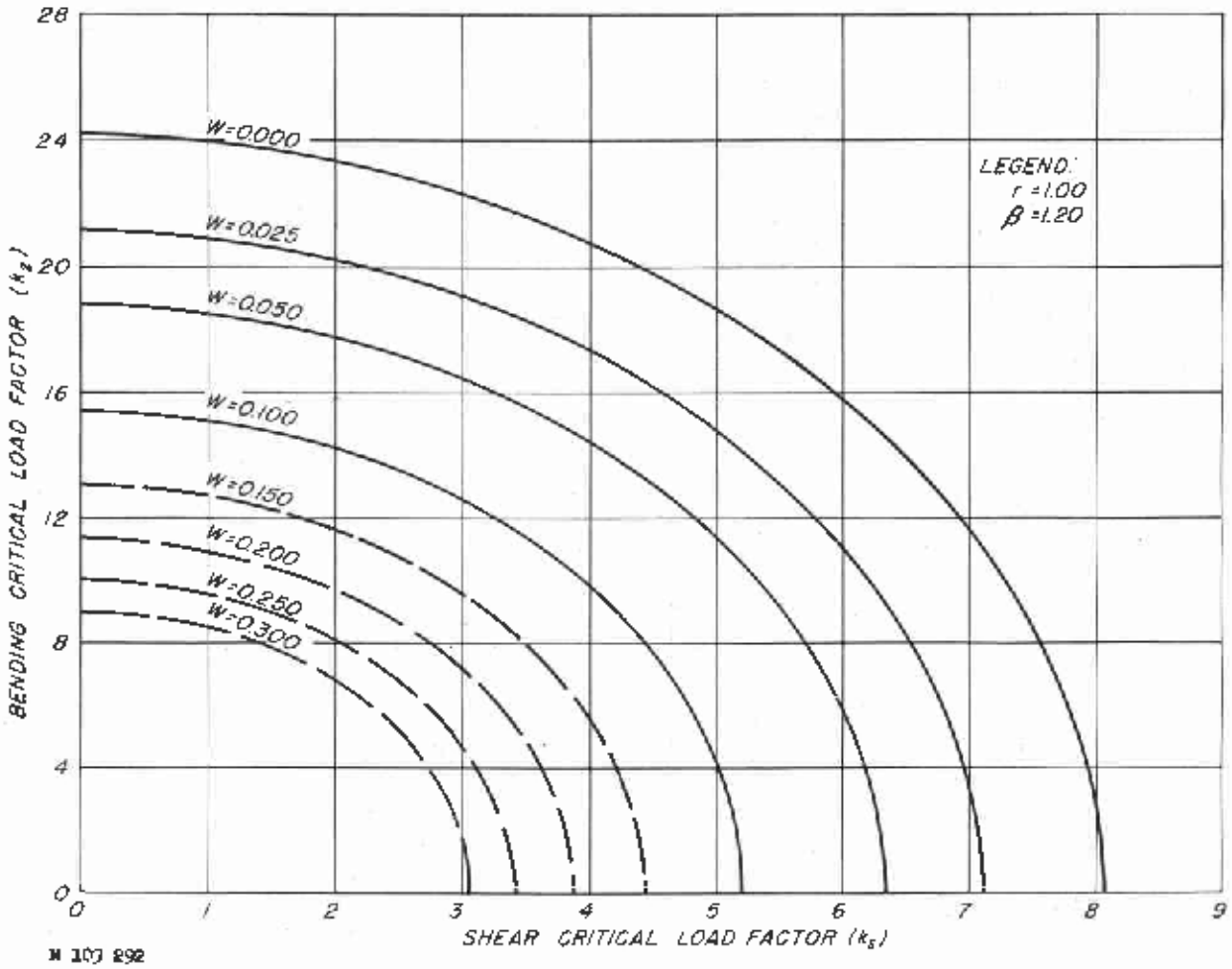


Figure 19. --Critical load factor $k_z$ versus critical load factor $k_s$ for $r = 1.00$, $\beta = 1.20$, and $0.00 \leq W \leq 0.300$. See figure 5 for notation. Dashed lines indicate computed results which are too high by more than 10 percent because of convergence behavior.

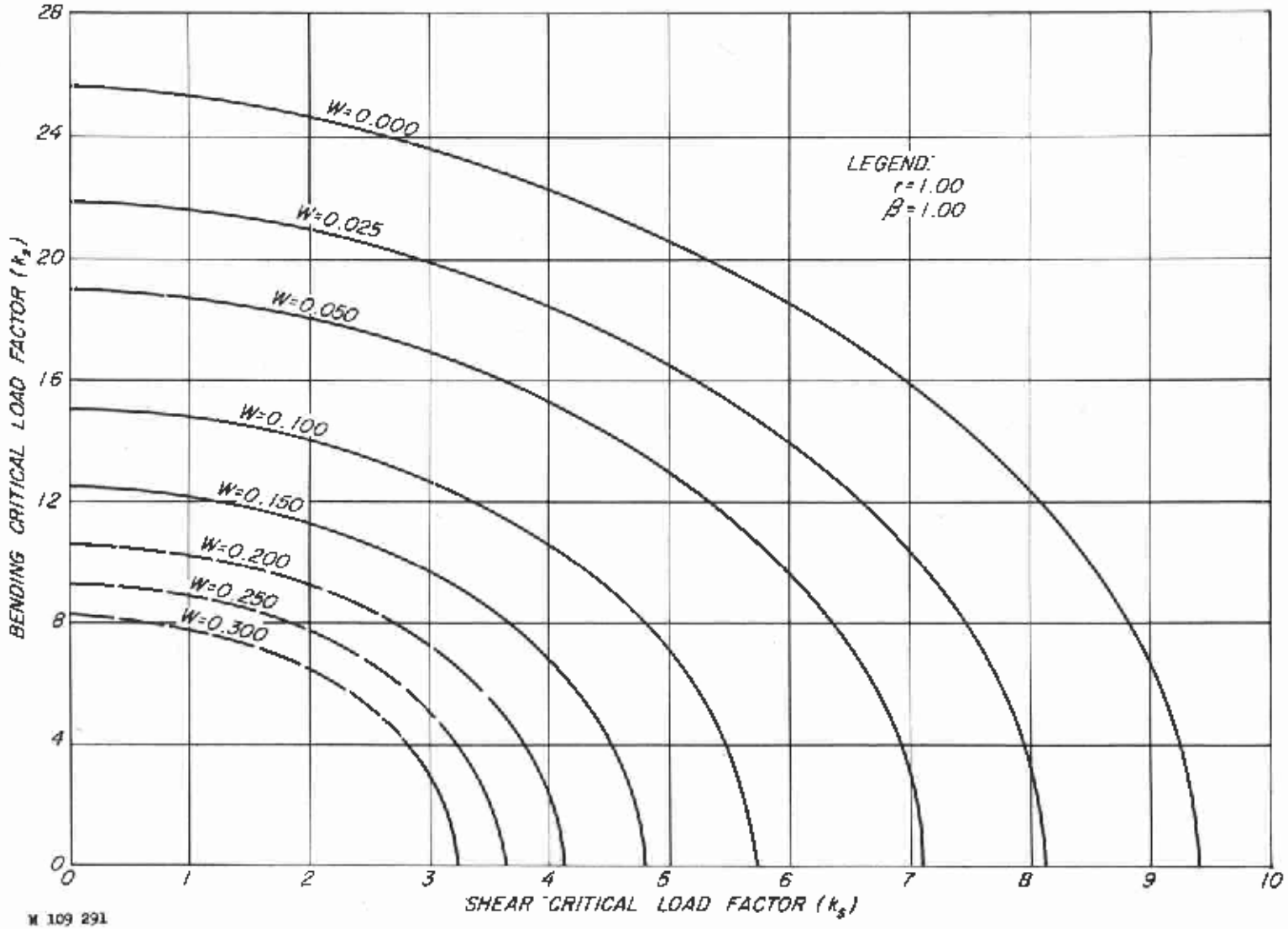


Figure 20.--Critical load factor $k_2$ versus critical load factor $k_s$ for $r = 1.00$, $\beta = 1.00$, and $0.00 \leq W \leq 0.300$. See figure 5 for notation. Dashed lines indicate computed results which are too high by more than 10 percent because of convergence behavior.

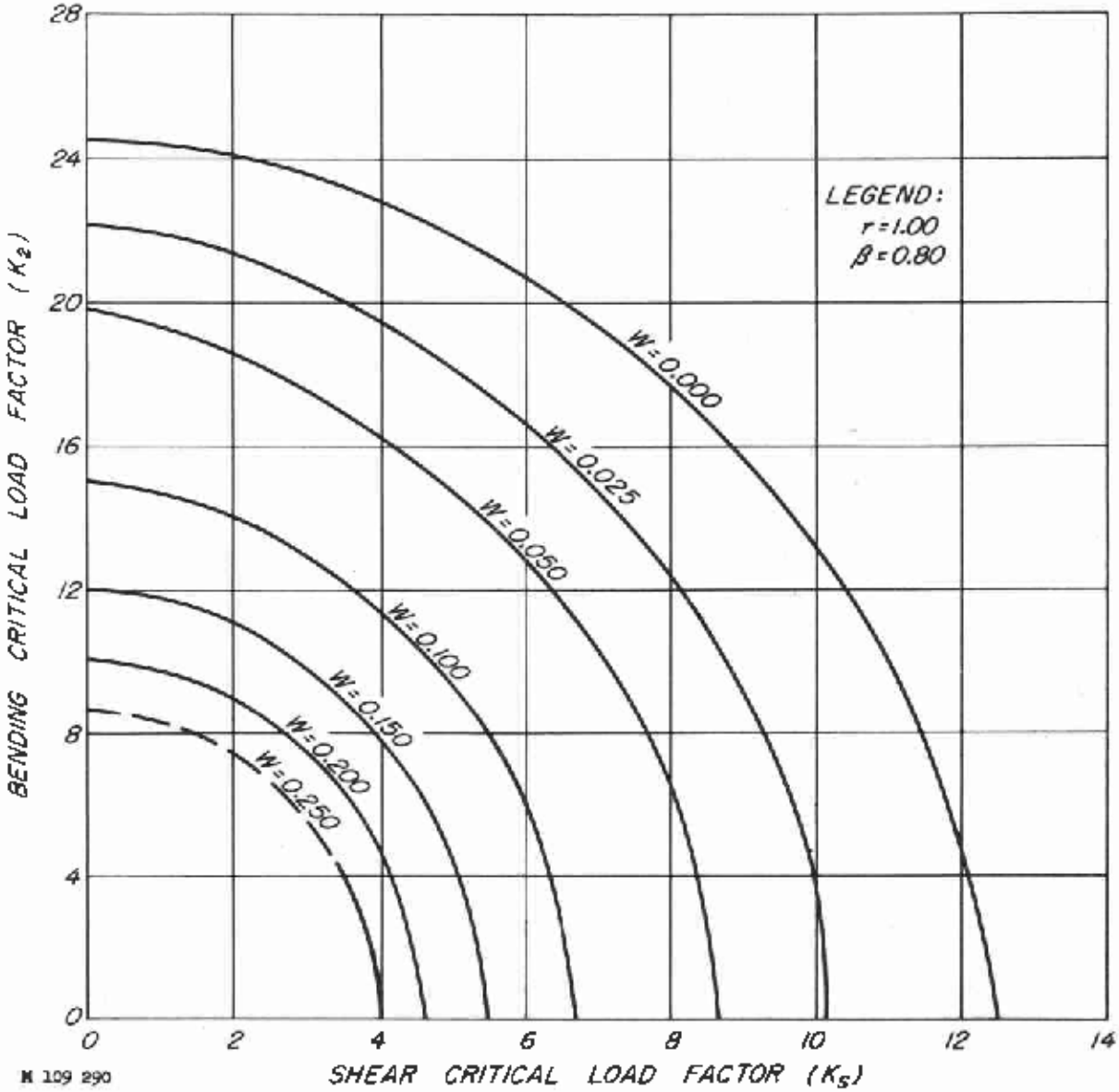


Figure 21.--Critical load factor $k_2$ versus critical load factor $k_s$ for $\underline{r} = 1.00$, $\underline{\beta} = 0.80$, and $0.00 \leq \underline{W} \leq 0.250$. See figure 5 for notation. Dashed lines indicate computed results which are too high by more than 10 percent because of convergence behavior.

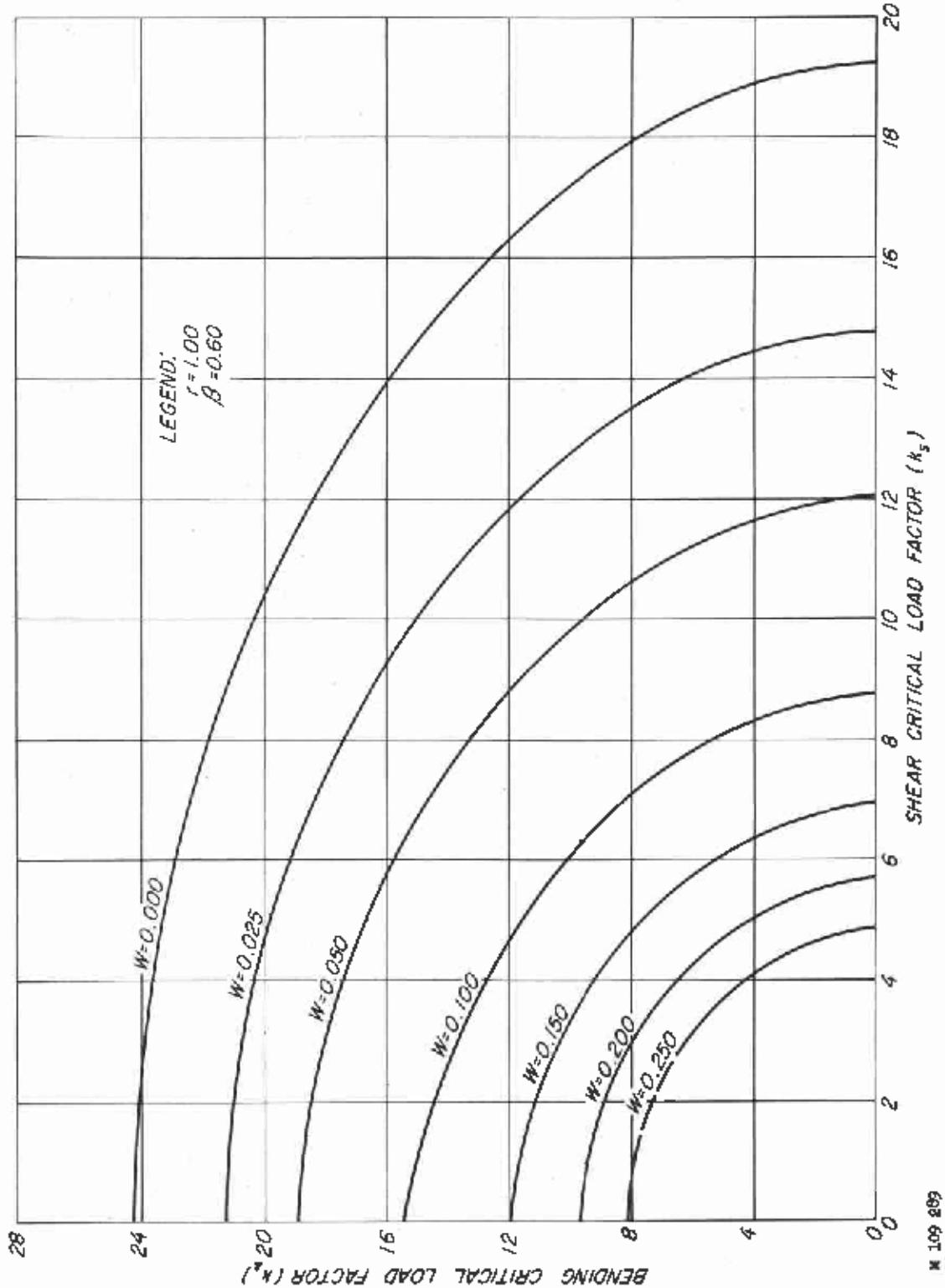


Figure 22.--Critical load factor $k_2$ versus critical load factor $k_s$ for $r = 1.00$, $\beta = 0.60$, and $0.00 \leq W \leq 0.250$. See figure 5 for notation. Dashed lines indicate computed results which are too high by more than 10 percent because of convergence behavior.

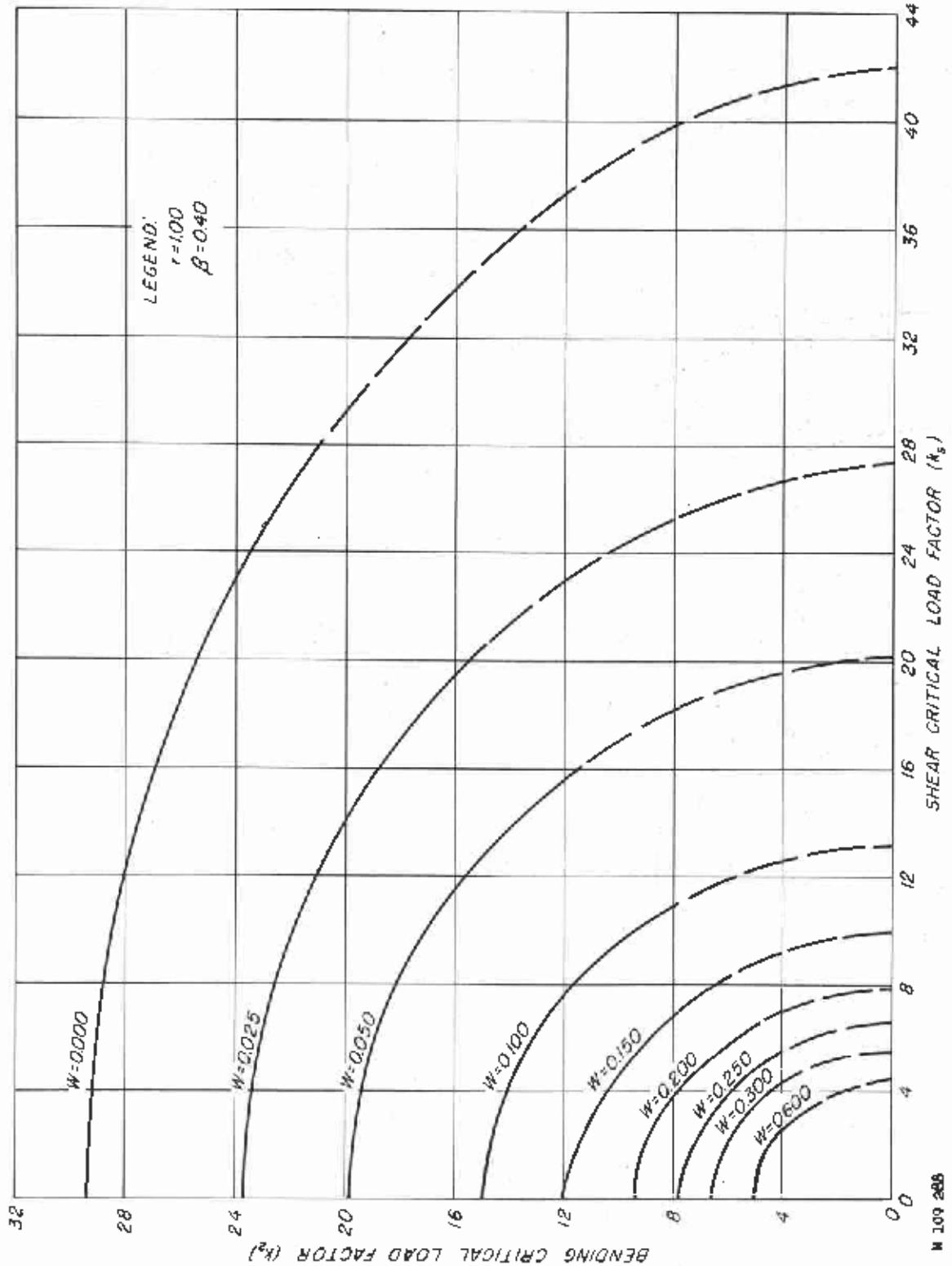


Figure 23.--Critical load factor $k_2$ versus critical load factor $k_s$ for $r = 1.00$, $\beta = 0.40$, and $0.00 \leq W \leq 0.600$. See figure 5 for notation. Dashed lines indicate computed results which are too high by more than 10 percent because of convergence behavior.

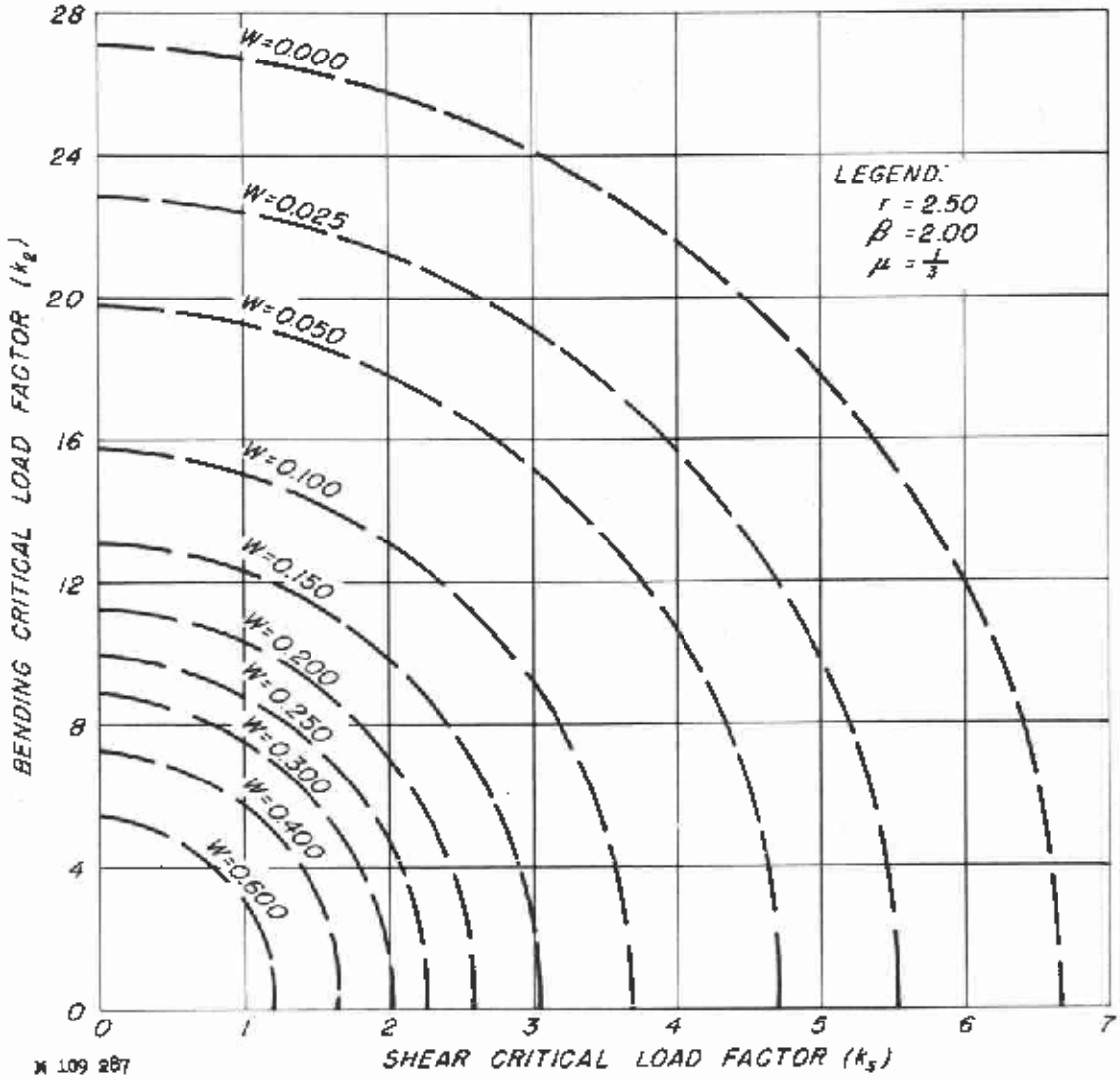


Figure 24.--Critical load factor $k_2$ versus critical load factor $k_s$ for $r = 2.50$, $\beta = 2.00$, and $0.00 \leqq W \leqq 0.600$. See figure 5 for notation. Dashed lines indicate computed results which are too high by more than 10 percent because of convergence behavior.

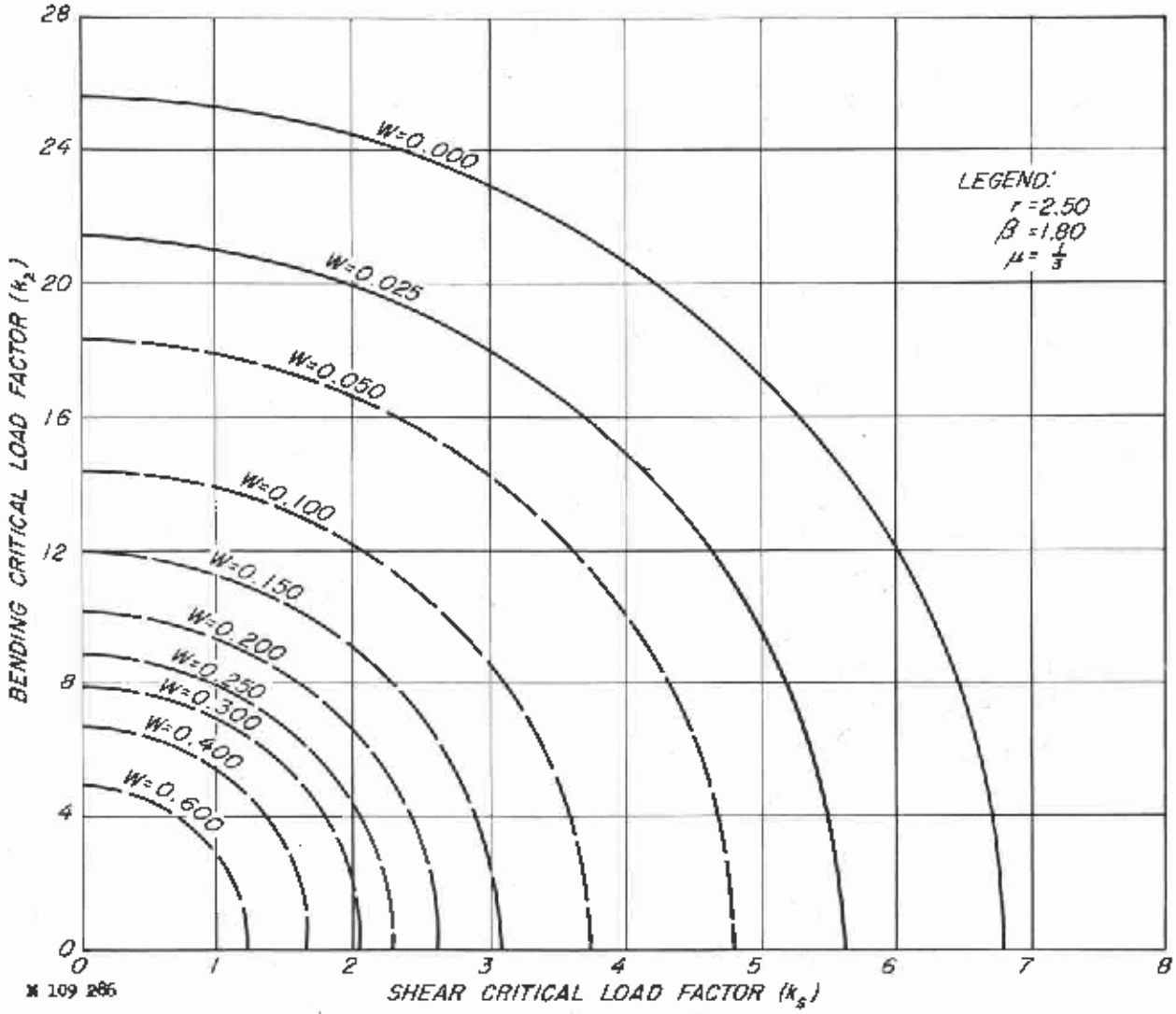


Figure 25.--Critical load factor $k_2$ versus critical load factor $k_s$ for $\underline{r} = 2.50$, $\underline{\beta} = 1.80$, and $0.00 \leq \underline{\overline{W}} = 0.600$. See figure 5 for notation. Dashed lines indicate computed results which are too high by more than 10 percent because of convergence behavior.

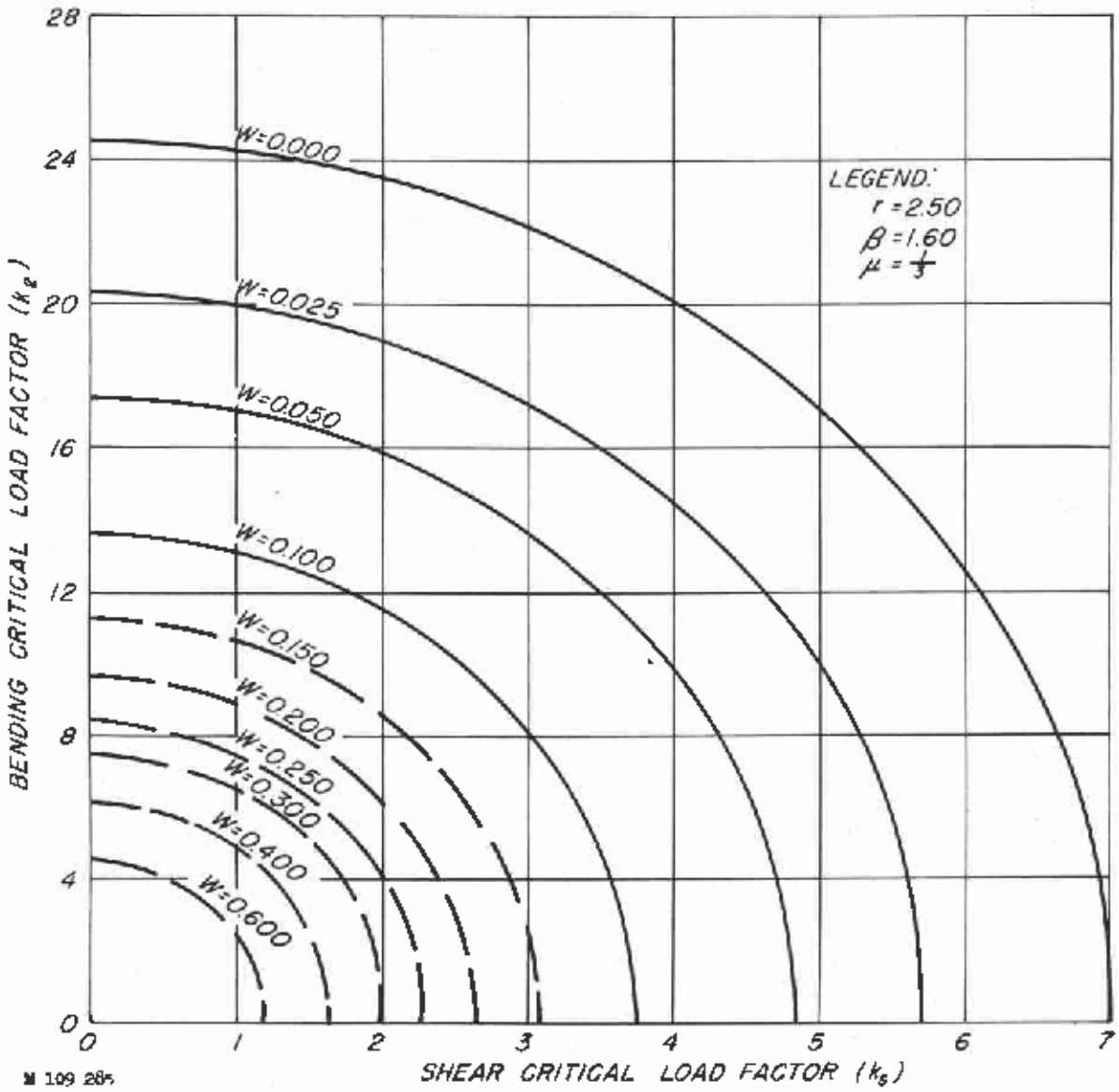


Figure 26.--Critical load factor $k_z$ versus critical load factor $k_s$ for $\underline{r} = 2.50$, $\underline{\beta} = 1.60$, and $0.00 \leqq \overline{W} \leqq 0.600$. See figure 5 for notation. Dashed lines indicate computed results which are too high by more than 10 percent because of convergence behavior.

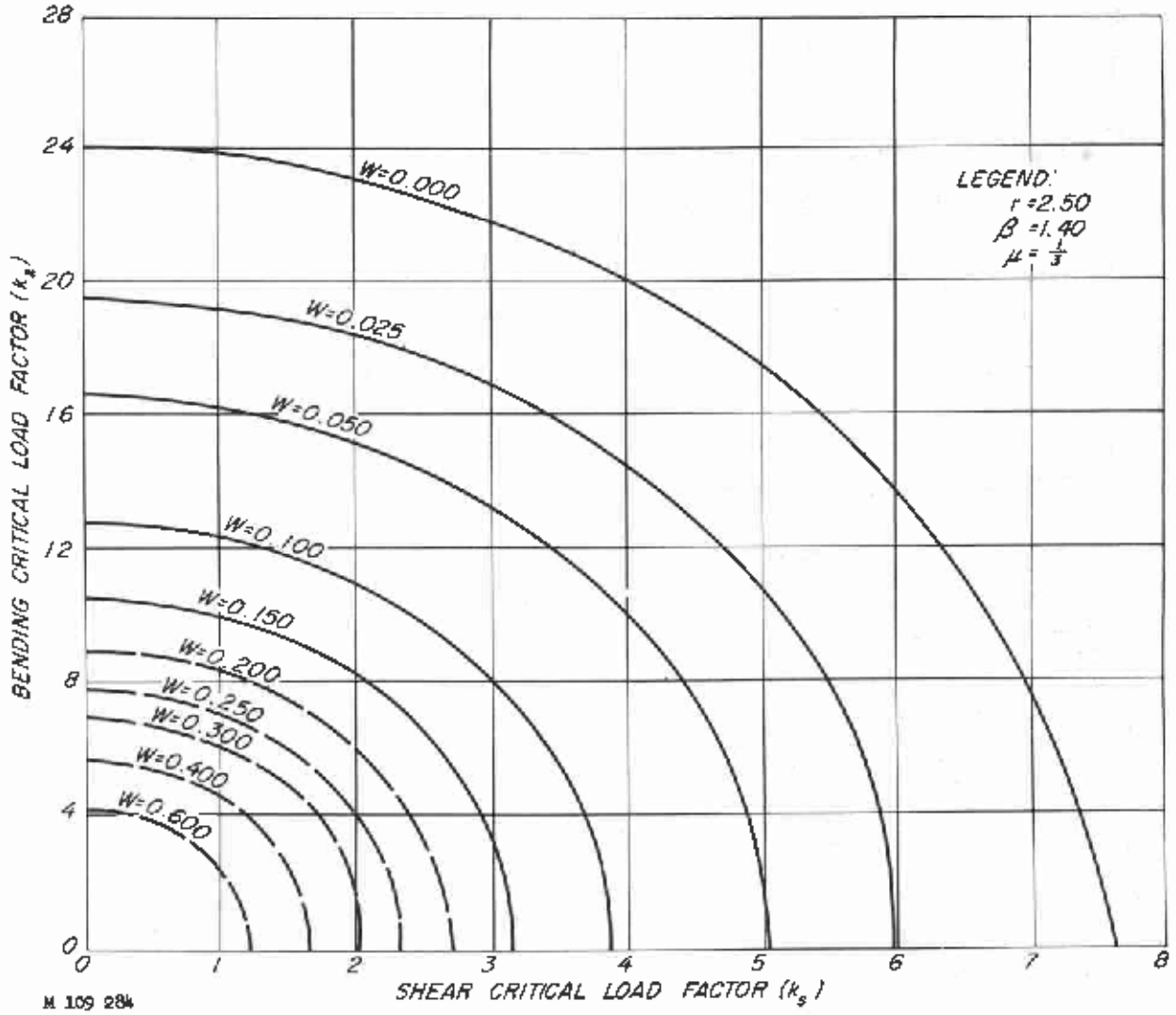


Figure 27. --Critical load factor $k_2$ versus critical load factor $k_s$ for $r = 2.50$, $\beta = 1.40$, and $0.00 \leqq W \leqq 0.600$. See figure 5 for notation. Dashed lines indicate computed results which are too high by more than 10 percent because of convergence behavior.

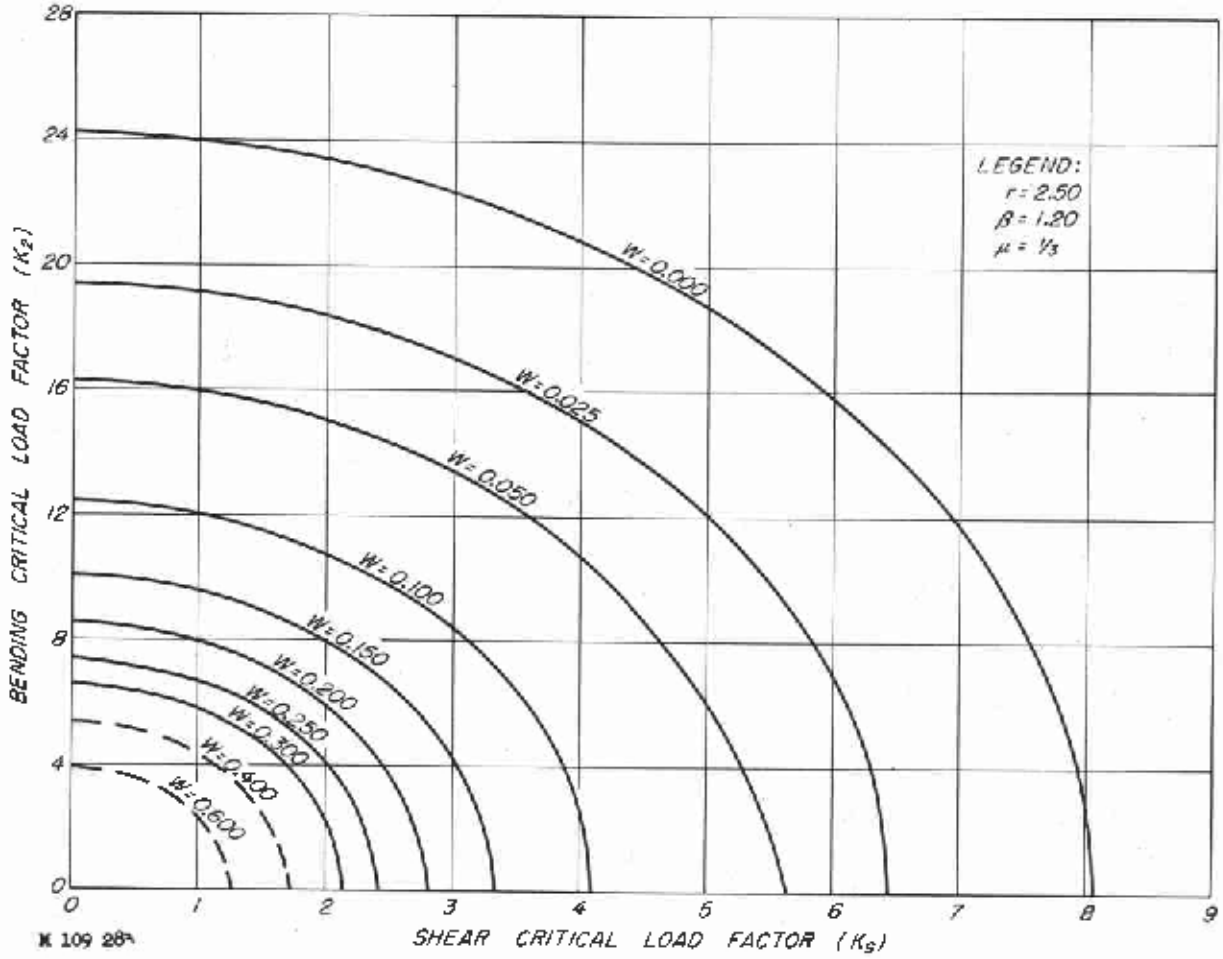


Figure 28.--Critical load factor $k_2$ versus critical load factor $k_s$ for $r = 2.50$, $\beta = 1.20$, and $0.00 \leqq W \leqq 0.600$. See figure 5 for notation. Dashed lines indicate computed results which are too high by more than 10 percent because of convergence behavior.

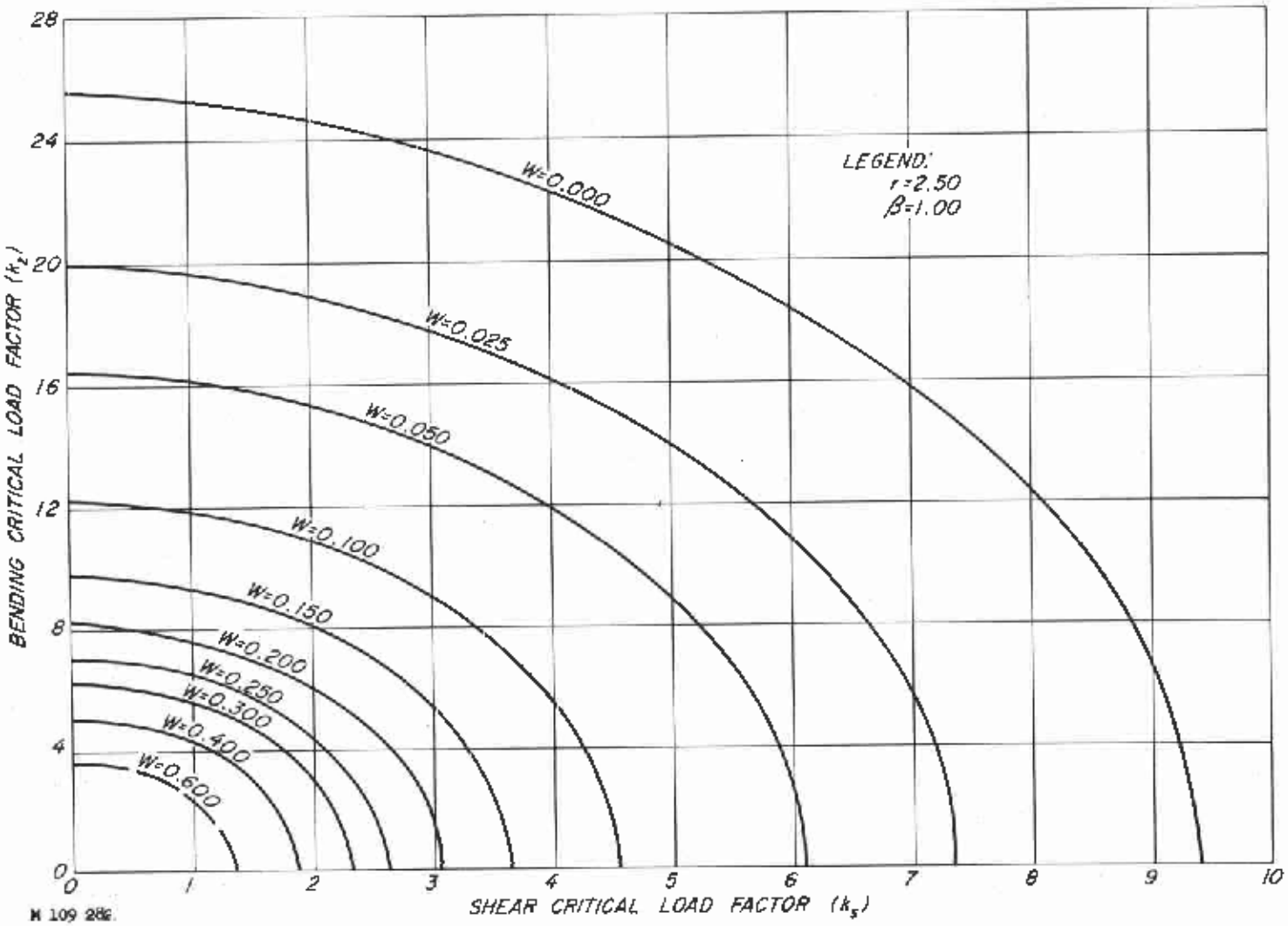


Figure 29. --Critical load factor $k_2$ versus critical load factor $k_s$ for $r$ = 2.50, $\beta$ = 1.00, and $0.00 \leq W \leq 0.600$. See figure 5 for notation. Dashed lines indicate computed results which are too high by more than 10 percent because of convergence behavior.

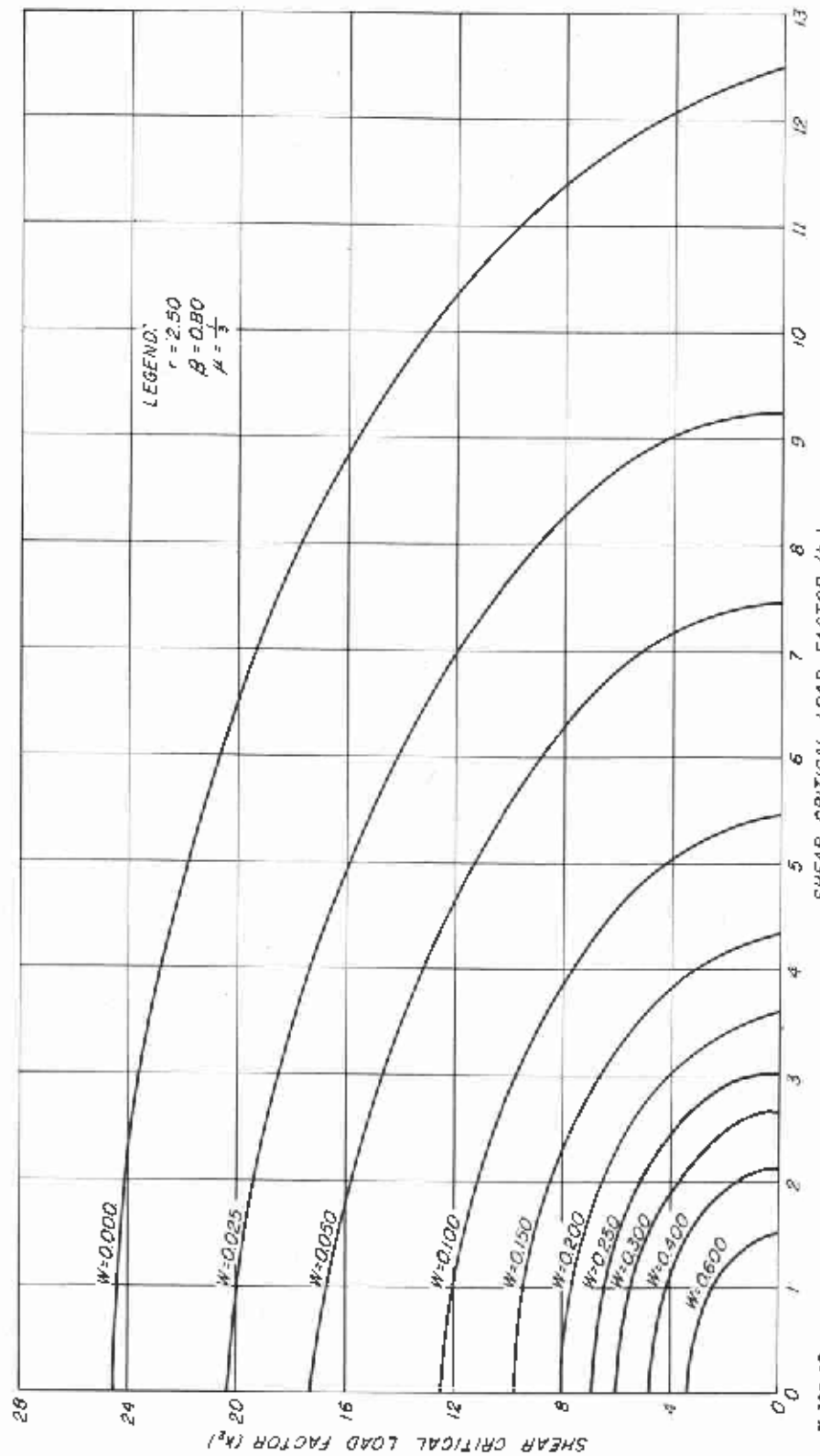


Figure 30.--Critical load factor $k_2$ versus critical load factor $k_s$ for $r = 2.50$, $\beta = 0.80$, and $0.00 \leq W \leq 0.600$. See figure 5 for notation.

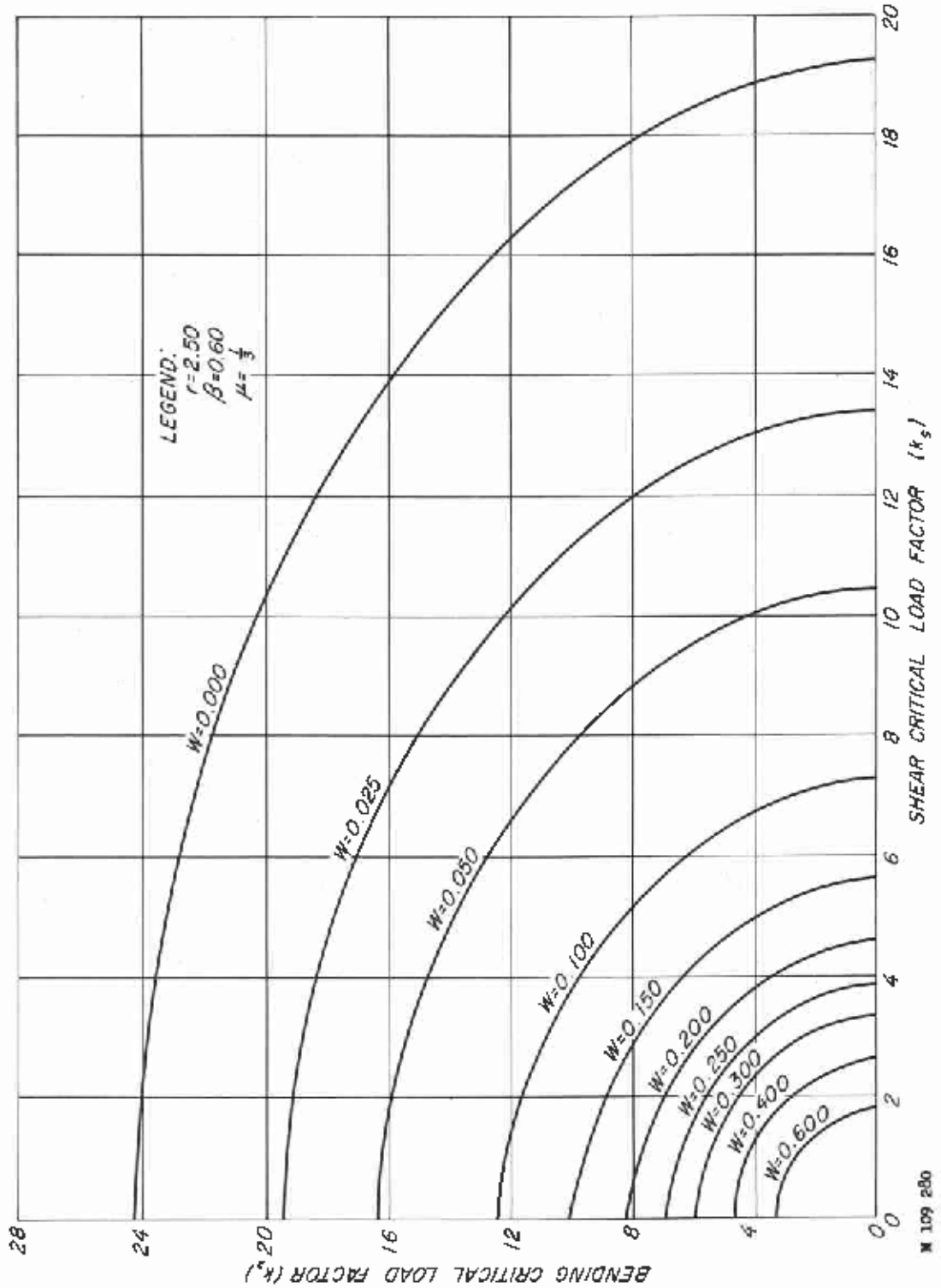


Figure 31.--Critical load factor $k_2$ versus critical load factor $k_s$ for $r = 2.50$, $\beta = 0.60$, and $0.00 \leq W \leq 0.600$. See figure 5 for notation.

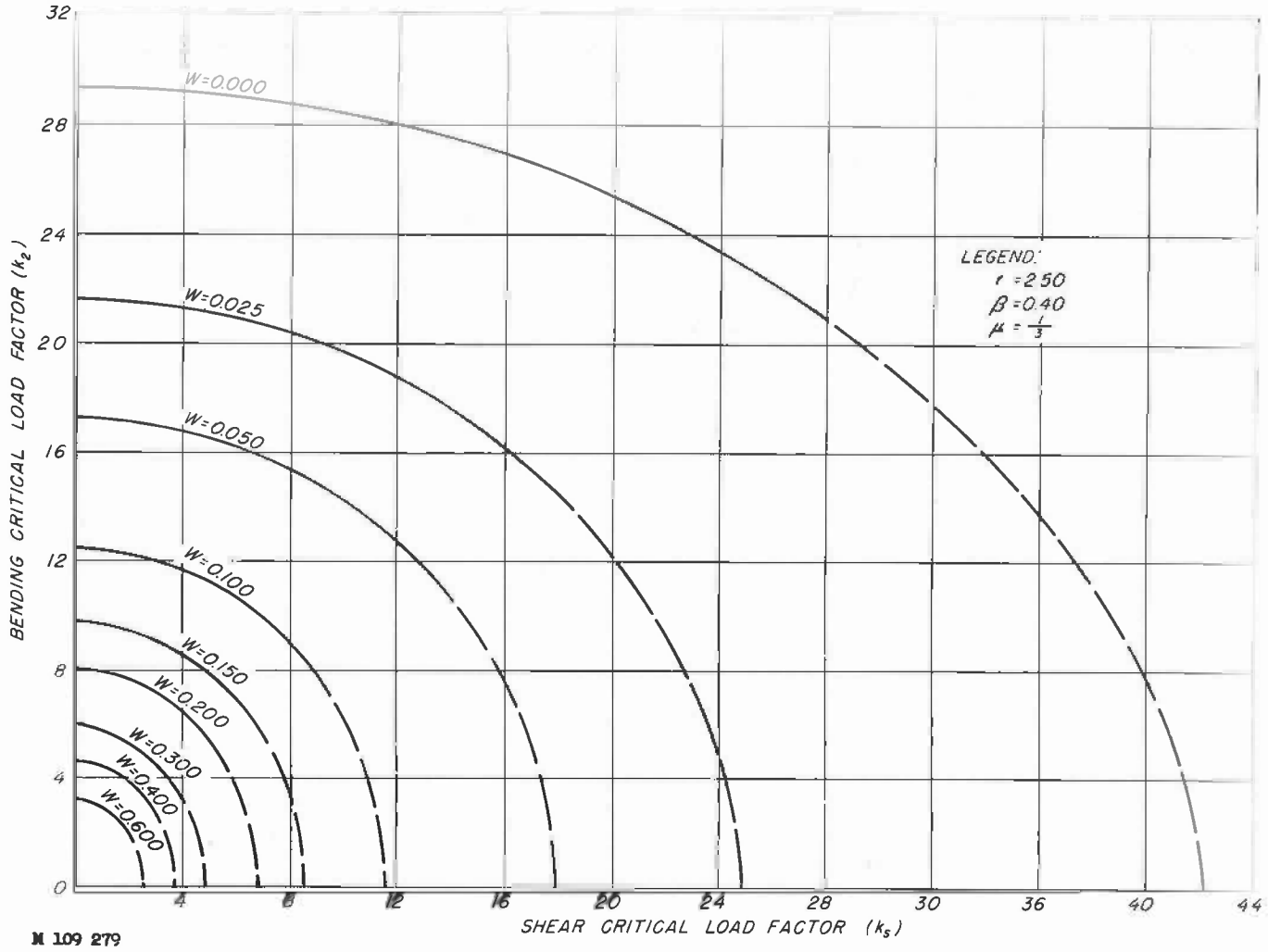


Figure 32. --Critical load factor $k_2$ versus critical load factor $k_s$ for $r = 2.50$, $\beta = 0.40$, and $0.00 \leq W \leq 0.600$. See figure 5 for notation. Dashed lines indicate computed results which are too high by more than 10 percent because of convergence behavior.



GPO 828868 - 2